Am J Nucl Med Mol Imaging 2013;3(1):44-56
www.ajnmmi.us /ISSN:2160-8407/ajnmmi1208007

Original Article

One-step and one-pot-two-step radiosynthesis of cyclo-RGD-^{18}F-aryltrifluoroborate conjugates for functional imaging

Ying Li[1], Jinxia Guo[2], Shiqing Tang[1], Lixin Lang[2], Xiaoyuan Chen[2], David M Perrin[1]

[1]*Department of Chemistry, University of British Columbia, 2036 Main Mall, Vancouver, B.C., V6T-1Z1, Canada;* [2]*Laboratory of Molecular Imaging and Nanomedicine (LOMIN), National Institute of Biomedical Imaging and Bioengineering (NIBIB), National Institutes of Health (NIH), 31 Center Drive, Suite 1C14, Bethesda, MD 20892-2281, USA*

Received August 23, 2012; Accepted September 22, 2012; Epub January 5, 2013; Published January 15, 2013

Abstract: Arylboronates capture aqueous ^{18}F-fluoride in one step to afford a highly polar ^{18}F-labeled aryltrifluoroborate anion (^{18}F-ArBF$_3^-$) that clears rapidly *in vivo*. To date however, there is little data to show that a ligand labeled with a prosthetic ^{18}F-ArBF$_3^-$ will provide functional images. RGD, a high-affinity ligand for integrins that are present on the cell surface of numerous tumors, has been labeled in many formats with many different radionuclides, and as such represents a well-established ligand that can be used to evaluate new labeling methods. Herein we have labeled RGD with a prosthetic ^{18}F-ArBF$_3^-$ via two approaches for the first time: 1) a RGD-boronate bioconjugate is directly labeled in one step and 2) an alkyne-modified arylborimidine is first converted to the corresponding ^{18}F-ArBF$_3^-$ which is then conjugated to an RGD-azide via Cu$^+$-mediated [2+3] dipolar cycloaddition in one pot over two steps. RGD-^{18}F-ArBF$_3^-$ bionconjugates were produced in reasonable radiochemical yields using low amounts of ^{18}F-fluoride anion (10-50 mCi). Despite relatively low specific activities, good tumor images are revealed in each case.

Keywords: One-step ^{18}F-labeling, click labeling, RGD, PET imaging

Introduction

Integrins, a class of surface receptors, are the major receptors, by which cells attach themselves to the extracellular matrices, and some of which are involved in cell-cell adhesion events [1]. They have been found to participate in various biological processes including embryonic development, cell activity mediation, regulation of the balance between cell proliferation and cell death, and cancer development [2]. One of the most recognized peptide motifs that bind to the $\alpha_v\beta_3$ receptor, which is found to be overexpressed in many cancer cell lines [3], contains the amino acid sequence: Arg-Gly-Asp (RGD) [3, 4], the discovery of which enabled the development of a wide range of RGD-based diagnostics and therapeutics [5-10]. Cyclopentapeptides with the RGD sequence have proven ideal ligands for molecular imaging to assist diagnosis, gauge the stage of cancers/tumor, and evaluate therapies and drugs. Accordingly, a great deal of beautiful imaging work has been reported recently by labeling RGD-peptides with a variety of radionuclides [11-13], fluorescent probes [14, 15], and contrast agents to locate the *in vivo* distribution of the $\alpha_v\beta_3$ receptor [16]. Radiometals such as ^{64}Cu, ^{68}Ga, and ^{111}In have also been used to radiolabel RGD-containing peptides [17-21].

Recognizing the importance of decreased lipophilicity of the ^{18}F-bearing prosthetic, Haubner and coworkers prepared ^{18}F-labeled galacto-*c*(RGDfK) by coupling 4-nitrophenyl 2-^{18}F-fluoropropionate to galacto-*c*(RGDfK) [22, 23]. Towards similar ends, Hatano and co-workers reported a one-step electrophilic radiofluoridation to prepare ^{18}F-*c*(RGDfMeV) with ^{18}F-acetylhypofluorite (^{18}F-AcOF), albeit at specific activities of <1 mCi/μmol [24]. Although several regioisomers were obtained during the radiosynthesis, the ^{18}F-*c*(RGDfMeV) peptides showed high affinity and specificity for the targeted inte-

grin. High tumor-to-blood/muscle ratios were obtained, however there was very high uptake of the radioactivity in the liver and kidney, and some in the bone. Chen *et al.* reported ^{18}F-labeled RGD with N-succinimidyl 4-^{18}Ffluorobenzoate to image brain tumor angiogenesis with an orthotopic U251T brain tumor model [25]. A high tumor-to-brain ratio was obtained with high receptor specificity for this radiotracer. Recently, *O*-(2-(2-^{18}F-fluoroethoxy)-ethyl)-*N*-methylhydroxyl amine [26] and/or 4-^{18}F-fluorobenzaldehyde [27] was regioselectively introduced onto the RGD-4C-derivatized analogues via either Michael addition or oxime formation. In each case, promising tumor uptake was reported. Taken together, these examples demonstrate that RGD-containing cyclic pentapeptides are robust diagnostic imaging agents. Over the past decade, numerous reports, as reviewed extensively [13, 16, 23, 26, 28-32], have featured many different approaches to label RGD. Indeed, new labeling methods with particular regards to facile one-step and one-pot reactions continue to be the subject of reports on labeled RGD [33-37]. Rapid and convenient labeling methods notwithstanding, concerns about prosthetic lipophilicity also continue to justify the development of modified RGDs through the incorporation of hydrophilic PEG linkers and glycosylated groups to decrease the tracer's hydrophobicity to favour circulation and excretion.

Recently, we conceived of a novel method whereby arylboronates capture *aqueous* ^{18}F-fluoride anion to afford an ^{18}F-labeled aryltrifluoroborate anion (^{18}F-ArBF_3^-) [38-40]. Labeling proceeds rapidly at room temperature and at acidic pH 2-3 to afford a water-soluble, non-coordinating, highly polar ArBF_3^- anion (log P_{ow} < -4 for the ArBF_3^- moiety). PET images of a biotinylated-^{18}F-ArBF_3^- demonstrated *in vivo* stability thereby highlighting their potential use in PET imaging [39]. Furthermore, the clinically trialed drug Marimastat was conjugated to a boronate via an amide bond and labeled directly at relatively low specific activities of 0.16 -0.39 Ci/μmol to reveal tumor associated matrix metalloprotease activity in breast cancer xenografts. Others have labeled Lymphoseek™ with pendant ^{18}F-ArBF_3^- groups and demonstrated excellent sentinel lymph node imaging at relatively low specific activity [41].

While PET images of tumors in animals [22, 42] and humans [29, 43, 44] have been acquired using ligands with specific activities in the range of 0.5 Ci/μmol, and even as low as 0.08-0.25 Ci/μmol [45-48], in the case of the Marimastat-^{18}F-ArBF_3^- conjugate, tumor differentiation was poor and images were plagued by very high background [34, 49]. Because RGD represents a powerful and reliable imaging agent that has been the subject of myriad reports, we hypothesized that an RGD-^{18}F-ArBF_3^- bioconjugate along with a visualization of functional images would validate the hypothesis that a highly polar, rapidly clearing ^{18}F-ArBF_3^-, when conjugated to a *bona-fide* ligand such as RGD, will provide excellent images. Moreover, because of the anionic character of the ^{18}F-ArBF_3^-, such a prosthetic greatly increases the hydrophilicity of the peptides to which it is attached, and therefore favors *in vivo* clearance and increases the chances for good tumour-to-blood ratios. To both simplify the synthesis and focus on verifying RGD-^{18}F-ArBF_3^- as a potential PET imaging agent, two monomeric RGD peptides (RGD-ArBF_3^-s) were prepared and their ^{18}F-labeling either in a single step or via a one-pot-two-step process to afford two different RGD-^{18}F-ArBF_3^- analogs is described herein. Preliminary tumor-specific images are presented to provide initial validation of this labeling method.

Materials and methods

Reagents and solvents were purchased from Fisher, Sigma-Aldrich, Alfa-Aesar, Novabiochem or Oakwood. All chemicals were used as supplied unless stated otherwise. The ^{18}F Trap & Release column (HCO_3^- form, ~ 10 mg) was purchased from ORTG, Inc. Deuterated solvents were obtained from Cambridge Isotope Laboratories. Analytical thin layer chromatography was undertaken on Silica Gel 60 F254 Glass TLC plates from EMD Chemicals and SiliaFlash F60 from Silicycle was used for flash chromatography. ESI-LRMS was performed on a Waters ZQ with a single quadrupole detector, attached to a Waters 2695 HPLC. ESI-HRMS were obtained on a Waters-Micromass LCT with a time-of-flight (TOF) detector. All NMR spectra were recorded at room temperature on a Bruker Avance 300 or 400 MHz spectrometer. Chemical shifts are reported using the δ scale in *ppm* and all coupling constants (*J*) are reported in hertz (Hz). Unless specified, ^{1}H NMR spec-

tra are referenced to the tetramethylsilane peak (δ = 0.00 *ppm*), ^{13}C NMR spectra are referenced to the chloroform peak (δ = 77.23 *ppm*), and ^{19}F NMR spectra are referenced to NEAT trifluoroacetic acid (δ = 0.00 *ppm*, -78.3 *ppm* relative to $CFCl_3$). HPLC analysis was performed on the Agilent 1100 HPLC system equipped with an auto-injector, a fraction collector and a diode array detector (non-radiolabeling) or on Waters 515 binary HPLC pump with a Waters 486 UV detector and a Bioscan Flow-Count detector (radiolabeling). Phenomenex Jupiter 10μ C18 300Å 4.6 mm × 250 mm column (Column I) was used for analysis or purification of the radiolabeling reaction and Agilent Eclipse XDB-C18 5μm 9.4 mm × 250 mm column (Column II) was used for semi-preparative HPLC.

Peptide syntheses

In general, RGD peptides were synthesized as linear precursors where the lysine amino group was either protected with the Dde group or first converted to the azide. Linear peptides were then cyclized to provide the cyclo-RGD whereupon the lysine was acylated with boronate or where the lysine-azide was used for Cu^+-mediated [2+3] cycloaddition. Briefly the following peptides and other components leading to the compounds were synthesized by a combination of standard solid phase and solution phase methods, purified either by standard flash silica chromatography or by HPLC when required, and characterized by ^{1}H-NMR and ^{19}F-NMR when possible and by ESI and HRMS: H-Asp(O^{t}Bu)-*D*-Phe-Lys(R)-Arg(Pbf)-Gly-OH (1a/b); *Cyclo*[Arg(Pbf)-Gly-Asp(O^{t}Bu)-*D*-Phe-Lys-(N_3)] (2a); *Cyclo*[Arg(Pbf)-Gly-Asp(O^{t}Bu)-*D*-Phe-Lys(Dde)] (2b); *Cyclo*[Arg-Gly-Asp-*D*-Phe-Lys(N_3)] (*c*[RGDfK(N_3)]) (3a); *Cyclo*[Arg(Pbf)-Gly-Asp(O^{t}Bu)-*D*-Phe-Lys] (3b); Mono-*tert*-butyl succinate; *Tert*-butyl 4-oxo-4-(4-tritylpiperazin-1-yl)butanoate (4); *Tert*-butyl 4-oxo-4-(piperazin-1-yl)butanoate (5); *Tert*-butyl 4-oxo-4-(4-(2,4,6-trifluoro-3-(4,4,5,5-tetraphenyl-1,3,2-dioxaborolan-2-yl) benzoyl)piperazin-1-yl)butanoate (6); 4-Oxo-4-(4-(2,4,6-trifluoro-3-(4,4,5,5-tetraphenyl-1,3,2-dioxaborolan-2-yl)benzoyl) piperazin-1-yl)butanoic acid (7); *Cyclo*[Arg(pbf)-Gly-Asp(O^{t}Bu)-*D*-Phe-Lys(suc-piperazinyl-boronate)] (8); *Cyclo*-[Arg-Gly-Asp-*D*-Phe-Lys(suc-piperazinyl-boronate)] (9); *Cyclo*[Arg-Gly-Asp-*D*-Phe-Lys(suc-piperazinyl-$ArBF_3^-$)] (10, also referred to RGD-SuPi-$ArBF_3^-$); 2,4,6-Trifluoro-3-(*1H*-naphtho[1,8-de] [1,3,2]diazaborinin-2(*3H*)-yl)benzoic acid (11); Alkyneborimidine (12) and details of their synthesis are found in the supporting information.

Radiosyntheses

Both RGD-SuPi-^{18}F-$ArBF_3^-$ and RGD-trAz-^{18}F-$ArBF_3^-$ were radiolabeled using 1-5 mCi of ^{18}F-fluoride anion that was supplemented with approximately 200-400 nmol of carrier ^{19}F-fluoride anion. For RGD-trAz-^{18}F-$ArBF_3^-$, the alkyne-modified arylborimidine was first converted to the corresponding ^{18}F-$ArBF_3^-$ according to the same method and then conjugated to the RGD-azide in the presence of copper ascorbate. Each labeling has been performed several times (n>4). Purification of each conjugate was achieved by HPLC. The same protocol was then applied for the production of both RGD species at relatively higher specific activity by using correspondingly higher levels of NCA ^{18}F-fluoride anion. These detailed protocols are indicated below.

Radiosynthesis of RGD-SuPi-^{18}F-$ArBF_3^-$ for animal imaging study

^{18}F-Fluoride anion (163 mCi, t= 0 min.) in ^{18}O-H_2O (400 μL) was combined with 1 M $NaHCO_3$ (6 μL) and CH_3CN (600 μL) in a 2 mL glass V-vial and evaporated at 105 ˚C over Ar flow. Following evaporation, the ^{18}F-fluoride anion was resuspended in a solution of 0.121 M KHF_2 (3 μL) to give an ^{18}F-fluoride anion cocktail. Of this cocktail, a volume of 2 μL was removed and transferred to a separate tube containing RGD-SuPi-boronate (100 nmol) that had been resuspended in CH_3CN (4 μL) and conc. HCl (0.5 μL). This tube was counted and found to contain 50 mCi and was assumed to contain two-thirds of the added carrier ^{19}F-fluoride. The resuspension of NCA ^{18}F-fluoride anion that had been dried in small volumes, has been problematic at times and therefore after resuspension of dried-down ^{18}F-fluoride anion, the tube into which the resuspended fluoride is always counted again to verify a) how much activity is actually resuspended and b) to calculate the specific activity of the ^{18}F-fluoride used. In this case the specific activity is 50 mCi/484 nmol or ~0.1 Ci/μmol. The acid catalyzed labeling reaction was allowed to react for 1 hour at room temperature. After 67 min., the reaction was quenched by the addition of 5% NH_4OH in 50%

aqueous EtOH (200 μL). Approximately one third of this quenched solution, (70 μL, 12.4 mCi) was removed and injected into an analytical column for HPLC for purification (Waters), column: Dionex Acclaim 300, C18, 3 mm, 300Å, 4.6 × 150 mm; HPLC Program 4: solvent A: 0.04 M HCO_2NH_4, solvent B: CH_3CN, 0 min. to 5 min., 0 % B to 5%, 5 min. to 10 min., 5% B to 20% B, 10 min. to 20 min., 20% B to 50% B, 20 min. to 25 min., 50% B to 100% B, 25 min. to 28 min., 100% B to 95% B, 28 min. to 30 min., 95% B to 5% B, 30 min. to 32 min., 5% B; flow rate: 1 mL/min.; and column temperature: room temperature). The fraction containing the desired product, which eluted between 13.5 min. and 15.0 min. was manually collected and found to contain 659 mCi at approximately 2 hours following the start of synthesis. This was then diluted with H_2O (8 mL) and loaded on a preactivated C18 Sep-Pak cartridge (Waters, 1cc, 100 mg). The cartridge was then washed with H_2O (8 mL) and EtOH was used to release the peptide in 50 μL per fraction. The major C18 fraction (338 μCi at 2.2 hours, SA= 0.164 Ci/μmol) was delivered for imaging. The final isolated yield, not corrected for decay, was 4% (because only one third of the reaction was purified, the yield is calculated as 0.65 mCi/16.33 mCi).

Preparation of RGD-trAz-^{18}F-ArBF$_3^-$ for animal imaging study (14)-

To 13 mCi of NCA ^{18}F-fluoride anion, that had been supplemented with 500 nmol ^{19}F-fluoride anion (2 μL, 0.125 M KHF_2), was added conc. HCl (0.5 μL) and the alkyneborimidine 12 in THF (4 μL). The reaction mixture was left for 77 min. at room temperature and quenched with 5% NH_4OH in 50% aqueous EtOH (10 μL) that contained c[RGDfK(N_3)] 3a (100 nmol). Then 0.6 M sodium ascorbate (6 μL) and 0.2 M $CuSO_4$ (6 μL) was added successively. The click reaction was incubated for approximately 40 minutes. The crude reaction, which was counted and found to contain 5.14 mCi, was then injected to HPLC for purification with the same C18 column and HPLC program for RGD-SuPi-^{18}F-ArBF$_3^-$. The desired product (883 μCi) was manually collected and diluted with H_2O (8 mL) for solid phase extraction. The fraction was then trapped on a pre-activated C18 sep-pak cartridge and the cartridge was washed with H_2O (8 mL). The compound was then eluted with EtOH (50 μL per fraction). The major C18 fraction, 506 μCi at 3.7 hours following the start of synthesis, SA= 0.06 Ci/μmol was delivered for imaging. The final, isolated radiochemical yield, not corrected for decay, was 6.8%.

Specific activity calculations

The specific activity of an ^{18}F-ArBF$_3^-$ is defined as Ci/μmol ^{18}F-ArBF$_3^-$. In order to determine the specific activity in this case we assumed that the amount of endogenous carrier ^{19}F-fluoride anion present in NCA ^{18}F-fluoride anion is negligible compared to the amount of carrier added. Hence, the specific activity of the carrier added ^{18}F-fluoride anion used in labeling is Ci used divided by mmol total fluoride anion. Because 3 atoms of fluorine condense with one arylboronate, the specific activity of the ^{18}F-ArBF$_3^-$ is triple that of the fluoride used in the reaction.

Octanol-water partition coefficient determination

RGD-SuPi-^{18}F-ArBF$_3^-$ was prepared as noted above using 1 mCi ^{18}F-fluoride. The product was isolated via HPLC chromatography, manually collected, desalted by solid phase extraction, eluted by EtOH flush, and concentrated by rotary evaporation. The product (approximately 20 μCi) was then redissolved in H_2O (170 μL). Of this solution (50 μL) was removed to which was added n-octanol (50 μL) in an Eppendorf tube. The resulting mixture was thoroughly vortexed for 5 minutes and then centrifuged for 10 minutes at 13k rpm. The top and bottom layers were carefully removed and placed in new tubes. From each layer an aliquot was removed (0.5 μL) was spotted on a silica gel plate. The plate was then dried, covered with polyethylene film (saran wrap), and stored in a phosphorimager cassette for 5 minutes. The phosphorimager screen was then scanned using the Typhoon Phosphorimager and ImageQuant software to record relative radiographic density in each spot which reflects the octanol-water partion. The direct ratio of the activity in octanol over radioactivity in water was found to be $1.6 \cdot 10^{-4}$ providing a $\log P_{ow}$ of -3.8.

PET imaging

Cell culture and animal models: All animal studies were conducted in accordance with the principles and procedures outlined in the Guide

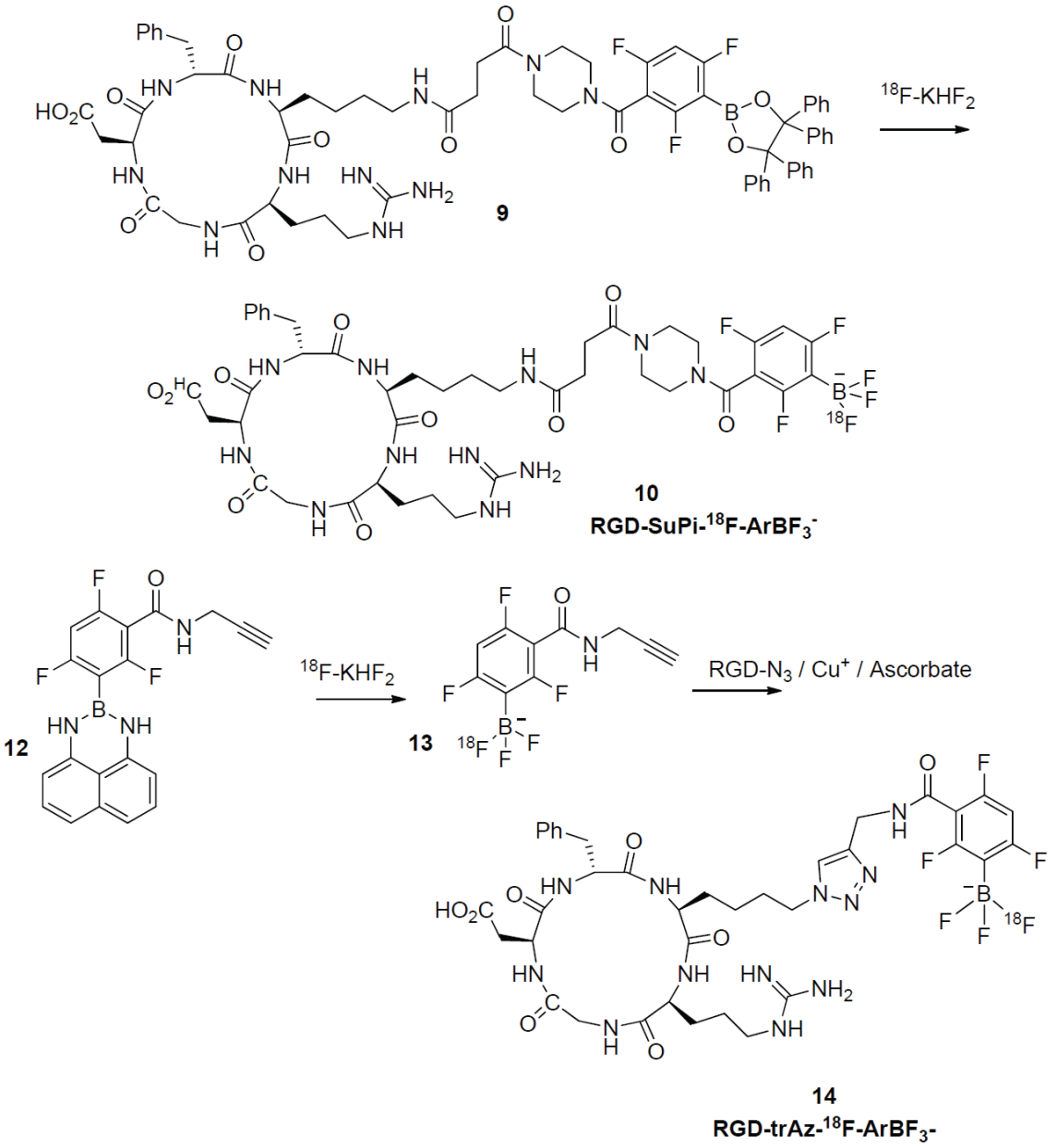

Figure 1. Synthetic scheme for the preparation of RGD-SuPi-^{18}F-ArBF$_3^-$ and RGD-trAz-^{18}F-ArBF$_3^-$: Above a tetraphenylpinacolate boronate ester conjugate to RGD is directly converted to the RGD-SuPi-^{18}F-ArBF$_3^-$ while below, the alkyne borimidine 12 is converted first to the corresponding ^{18}F-ArBF$_3^-$ alkyne 13 in situ, which is then directly conjugated to the RGD-azide to provide RGD-trAz-^{18}F-ArBF$_3^-$.

for the Care and Use of Laboratory Animals and were approved by the Institutional Animal Care and Use Committee of Clinical Center, NIH. The human glioblastoma U87MG cell line was purchased from the American Type Culture Collection (ATCC) and grown in MEM medium supplemented with 10% fetal bovine serum (FBS), 100 IU/mL penicillin, and 100 μg/mL streptomycin (Invitrogen) in a humidified atmosphere containing 5% CO_2 at 37°C. The U87MG xenograft tumor models were developed in 5 to 6week old female athymic nude mice (Harlan Laboratories) by injection of 5×10^6 cells in the right shoulders. Tumor growth was monitored using caliper measurements of perpendicular axes of the tumor. The tumor volume was estimated by the formula: tumor volume = a× (b^2) / 2, where a and b were the tumor length and

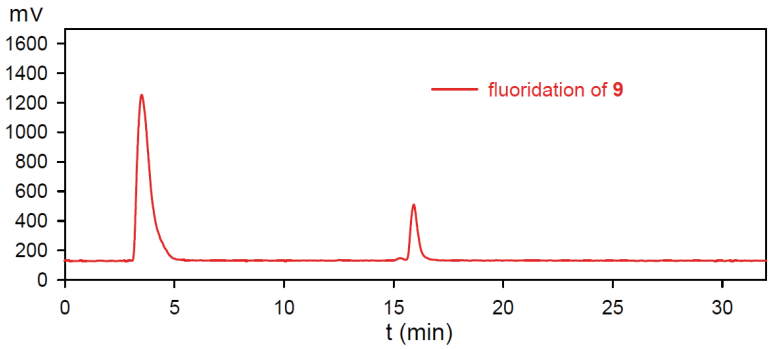

Figure 2. The radio-HPLC traces of the one-step ^{18}F-fluoridation of RGD-boronates: The HPLC trace represented the ^{18}F-fluoridation of RGD-SuPi-boronate 9.

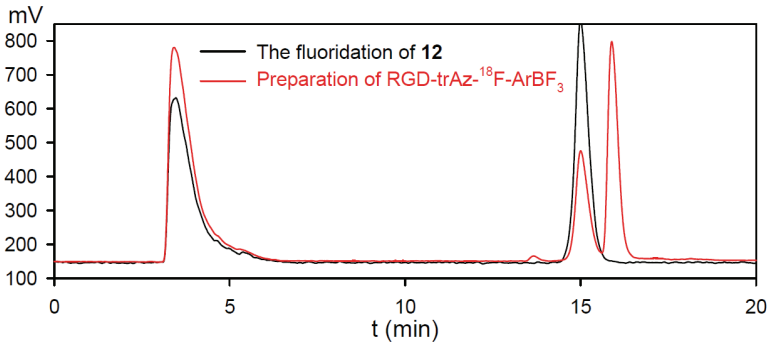

Figure 3. The HPLC traces of the one-pot two-step labeling reaction to prepare RGD-trAz-^{18}F-ArBF$_3^-$.The black trace was for the crude fluoridation reaction of 12 to prepare alkyne-^{18}F-ArBF$_3^-$ and the red trace was for the click reaction between the crude alkyne-^{18}F-ArBF$_3^-$ and c[RGDfK(N$_3$)].

width, respectively, in millimeters. The mice underwent small-animal PET studies when the tumor volume reached 100–300 mm^3 (3–4 weeks after inoculation).

MicroPET imaging

PET scans and image analysis were performed using an Inveon microPET scanner (Siemens Medical Solutions). Approximately 100 μCi of RGD-SuPi-^{18}F-ArBF$_3^-$ or RGD-trAz-^{18}F-ArBF$_3^-$ in 100 μL of saline was administered *via* tail vein injection under isoflurane anesthesia. Five-minute static PET images were acquired at 30 and 60 min. post-injection (n = 3/group). The images were reconstructed using a two-dimensional ordered-subset expectation maximization (2D OSEM) algorithm without correction for attenuation or scattering. For each scan, regions of interest (ROIs) were drawn over the tumor and muscle region using vendor software (ASI Pro 5.2.4.0) on decay-corrected whole-body coronal images. The radioactivity concentrations (accumulation) within the tumors and muscle were obtained from mean pixel values within the multiple ROI volume and then converted to MBq/mL/min. using the calibration factor determined for the Inveon PET system. These values were then divided by the administered activity to obtain (assuming a tissue density of 1 g/mL) an image-ROI-derived percent injected dose per gram (%ID/g).

Results

This work was primarily undertaken to demonstrate both one-step and one-pot-two-step aqueous RGD labeling and to validate this method through *in vivo* images. We chose RGD because it is known to give excellent tumor images, even at low specific activity. To do this we synthesized two variations of RGD that would enable the synthesis and validation of ^{18}F-labeling accordingly. These are shown in **Figure 1**; in the first case, labeling proceeds directly via acid catalyzed displacement of the tetraphenylpinacolate ester of boron 9 to give the corresponding RGD-SuPi-^{18}F-ArBF$_3^-$ 10 while in the second case, an alkyne-modified borimidine 12 is first converted to the corresponding alkyne-modified ^{18}F-ArBF$_3^-$ 13 that is not isolated but which is then condensed with an RGD-azide by Cu$^+$-catalyzed [2+3] cycloaddition to give the triazole linked RGD-trAz-^{18}F-ArBF$_3^-$ 14. In each case there is only one ^{18}F-fluorine atom on the ^{18}F-ArBF$_3^-$ and this is noted for clarity. The three fluorine atoms on the aryl ring are not displaced and are present to stabilize the ^{18}F-ArBF$_3^-$ against solvolysis.

Radiosynthesis prior to imaging

The fluoridation of RGD-boronate 9 was undertaken under the similar conditions as reported earlier [34]. HCO_2NH_4/CH_3CN HPLC solvent sys-

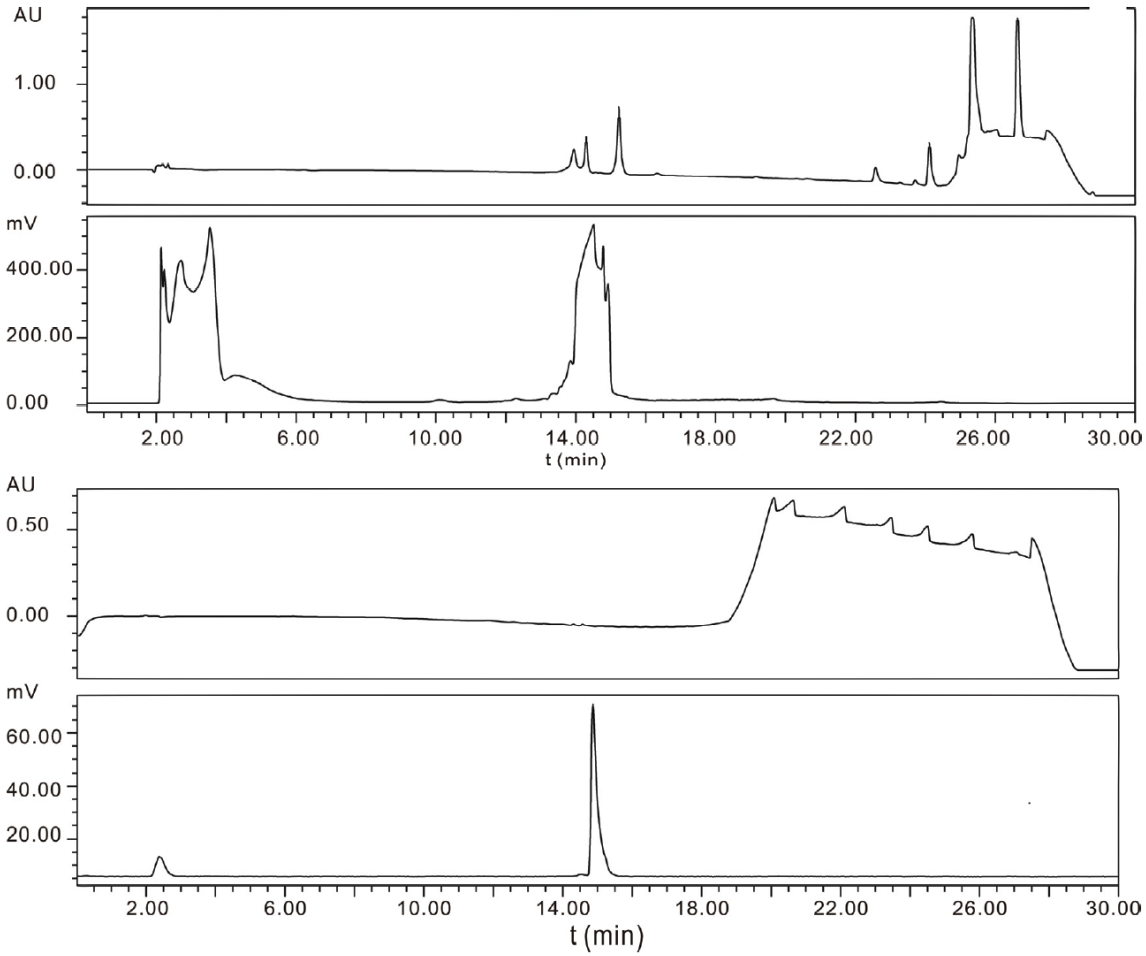

Figure 4. The HPLC traces for the preparation of RGD-SuPi-^{18}F-ArBF$_3^-$ used in Imaging: (top – crude reaction trace: UV and radiotrace, bottom - analytical re-injection of purified material: UV and radiotrace.

tem was found to be quite suitable for the HPLC analysis of the corresponding ^{18}F-ArBF$_3^-$s. The unlabeled standard of RGD-SuPi-ArBF$_3^-$ 10 was analyzed via ESI-LCMS with the desired masses of [M]$^-$: 996.3 and [M-HF]$^-$: 976.5 for RGD-SuPi-ArBF$_3^-$ 10 (t_R = 16.2 min., using Column I and HPLC Program 4 in the Agilent HPLC system). Because low levels of activity were used, the radiofluoridation of RGD-boronate 9 was carried out under carrier-added conditions that require approximately 200-300 nmol of total fluoride anion. Similarly, CH_3CN was used as the aqueous cosolvent while HCl was used to acidify the system with 5 equivalents of carrier fluoride added to drive the fluoridation forward. Each reaction was undertaken at room temperature for one hour and then quenched with 5% NH_4OH in 50% aqueous EtOH prior to the HPLC injection for analysis. The fluoridation was very reproducible ($n \geq 4$), and an average radiochemical yield of 10-15% was achieved using 1-5 mCi ^{18}F-fluoride anion as shown in **Figure 2**.

Through this work, we appreciated that arylboronic acids, or arylboronates that are modified with acid-labile protecting groups, provide much faster fluoridation rates (data not shown). Hence, we produced a 1,8-diaminonaphthalene (dan) protected borimidine-alkyne that rapidly fluoridated with radiochemical yields of ~30% within ~ 30 min. at room temperature. The reaction was quenched with ammonium hydroxide and directly used for a subsequent copper (I) catalyzed [2+3] cycloaddition reaction, which proved very efficient for conjugating the ^{18}F-ArBF$_3^-$ prosthetics into RGD. To compare this one-pot-two-step radiolabeling strategy for the incorporation of an ^{18}F-ArBF$_3^-$ with the one-step labeling method, *c*[RGDfK(N$_3$)] 3a was prepared and conjugated to the alkyne-^{18}F-ArBF$_3^-$

13 via the copper(I) catalysis for *in vivo* imaging. Briefly, the fluoridation of borimidine 12 was undertaken under the similar conditions for ~ 24 min. to provide the alkyne-^{18}F-ArBF_3^- intermediate 13 in a radiochemical yield of ~ 44%. The crude was then quenched with 5% NH_4OH/50% aq. EtOH, to which was added the RGD-azide and $CuSO_4$/sodium ascorbate to induce cycloaddition to give ^{18}F-labeled 14. Following room temperature reaction for ~30 min., the crude reaction was injected into an analytical HPLC column. The HPLC results were shown in **Figure 3**. As observed below, the intermediate alkyne-^{18}F-ArBF_3^- was not completely converted to the final product in this case yet provided sufficiently promising yields for us to contemplate animal imaging.

Radiosyntheses for animal imaging

For animal imaging, we used slightly higher levels of activity, 50 mCi and 13 mCi respectively in the radiosynthesis of RGD-SuPi-^{18}F+-ArBF_3^- or RGD-trAz-^{18}F-ArBF_3^- and consequently this enabled us to obtain radiotracers at respectable specific activities. Nevertheless, because much more radioactivity was loaded into an analytical column for purification, signal saturation was observed in the radiotraces as shown in **Figure 4**. Fortunately, free ^{18}F-fluoride anion and the desired RGD-SuPi-^{18}F-ArBF_3^- 10 are readily separated by this method which affords a radiochemically pure desired product (the small amount of free ^{18}F-fluoride anion observed in the analytical reinjection trace is attributed to residual free ^{18}F-fluoride anion in the injector loop) as shown in **Figure 4**. Using a simple solid phase extraction, ammonium formate and CH_3CN were successfully removed while a small amount of EtOH was used to release the product for formulation with saline buffer. The sample was then delivered for animal imaging.

In order to improve the yield of RGD-trAz-^{18}F-ArBF_3^- in the [2+3] cycloaddition step for use in animal imaging, concentrations of the reaction components were increased. As with the preparation of RGD-SuPi-^{18}F-ArBF_3^-, the entire crude reaction was applied to an analytical column and similarly the detector was saturated due to the large amount of radioactivity injected, as seen in **Figure 5**. Nevertheless, the desired product was easily isolated from free ^{18}F-fluoride anion and carefully separated from the intermediate alkyne-^{18}F-ArBF_3^-. Following solid phase extraction, the product was reanalyzed for purity on the same column and then delivered for animal imaging. Again, while this time there appeared to be considerable amount of free fluoride in the analytical QC control injection (**Figure 5**), this was attributed to the presence of free ^{18}F-fluoride anion in the injection loop or in the HPLC as otherwise there would have been considerable amount of bone signal in the images (*vide infra*). The overall isolated radiochemical yield in this step was approximately 6.8%.

Animal imaging

Representative coronal microPET images of U87MG tumor bearing mice at different times after intravenous injection of 100 μCi of RGD-SuPi-^{18}F-ArBF_3^- or RGD-trAz-^{18}F-ArBF_3^- are shown in **Figure 6**. The U87MG tumors were clearly visible with both imaging RGD analogs. The tumor uptake was 2.17 ± 0.76 %ID/g with RGD-SuPi-^{18}F-ArBF_3^- and 2.04 ± 0.43 %ID/g with RGD-trAz-^{18}F-ArBF_3^- at 30 min. post-injection. At 60 min. post-injection, the tumor uptake decreased to 1.51 ± 0.27 %ID/g with RGD-SuPi-^{18}F-ArBF_3^- and 1.17 ± 0.20 %ID/g with RGD-trAz-^{18}F-ArBF_3^-. There is no significant difference as to the tumor uptake with both tracers at both time points ($p > 0.05$). However, images with RGD-trAz-^{18}F-ArBF_3^- showed lower background compared with that with RGD-SuPi-^{18}F-ArBF_3^-. The tumor/muscle ratios with RGD-SuPi-^{18}F-ArBF_3^- are significantly lower than that with RGD-trAz-^{18}F-ArBF_3^- (3.88 vs. 8.16 at 30 min. post-injection, $p< 0.01$; 4.08 vs. 7.80 at 60 min. post-injection, $p< 0.01$). Bone uptake appeared to be minimal in both scans and this is discussed below. Because the mice were to be used for other experiments, they were not sacrificed for *post mortem* biodistribution analysis.

Discussion

Two labeling strategies were investigated in this work to radiolabel cyclic pentapeptides containing the RGD sequence. The fluoridation was carried out under acidic aqueous conditions at room temperature. The acid labile 1,8-diaminonaphthalene protected borimidine demonstrated faster and more efficient fluoridation than the tetraphenylpinacolate ester. Whereas the one-step labeling of RGD-SuPi-boronate gave an isolated radiochemical yield of 4%, the

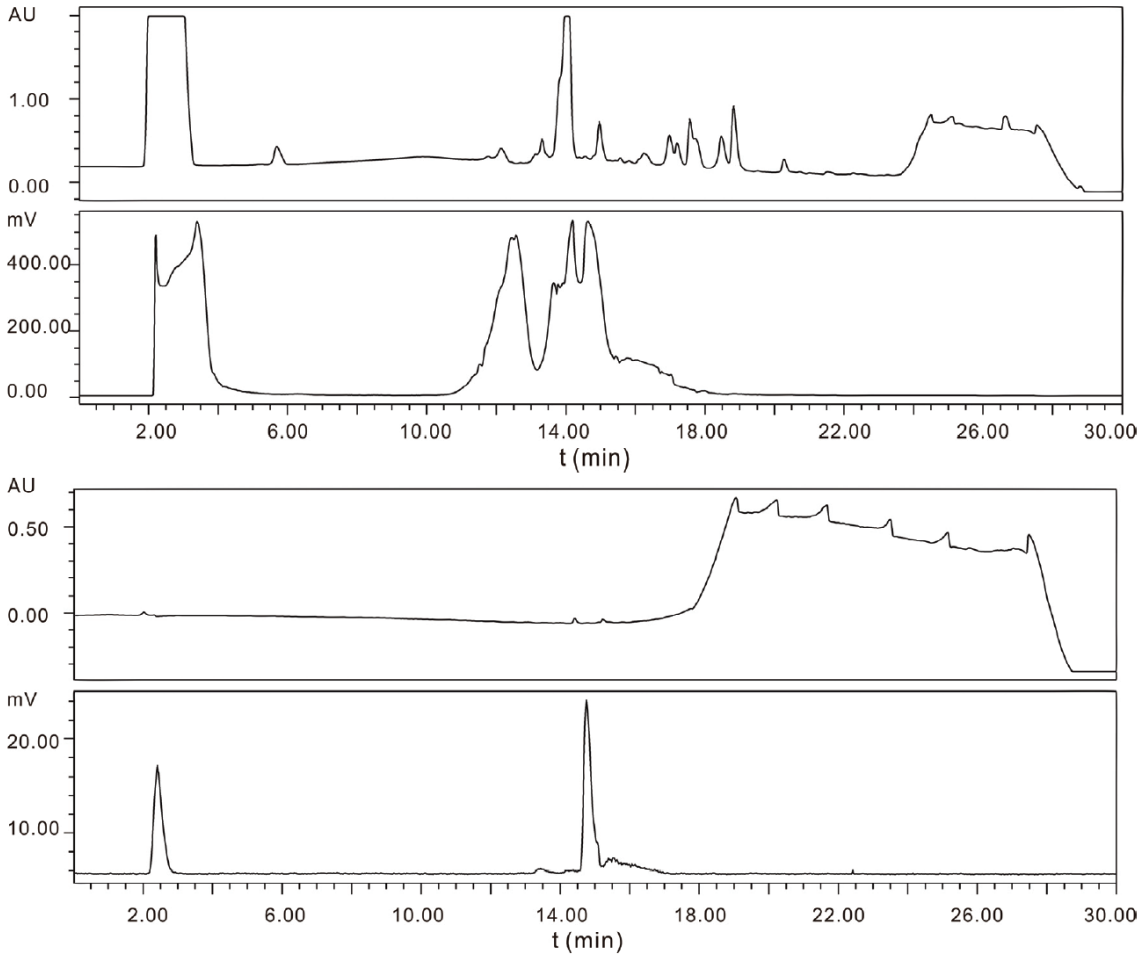

Figure 5. The HPLC traces for the preparation of RGD-trAz-^{18}F-ArBF$_3^-$. (top – crude reaction trace: UV and radiotrace, bottom - analytical re-injection of purified material: UV and radiotrace.

preparation of RGD-trAz-^{18}F-ArBF$_3^-$ gave an isolated radiochemical yield of 6.8%. These yields are reported for the syntheses that were performed on the day of imaging and these are found to be somewhat lower than we have seen in our hands. Notably, we performed preliminary labeling at the Triumf facility, while the radiosyntheses for animal imaging were performed at the NIH. While we do not have an immediate explanation for this, it is possible that differences in pH due to the presence carbonate from the anion exchange resin, or column differences could have resulted in lower yields.

The microPET images shown in **Figure 6** clearly indicated tumor uptake of the radiotracers. For both radiotracers, the *in vivo* clearance was rapid as most of the radiotracer cleared from the body within 60 min. Nevertheless, the rather rapid clearance reflects the considerable polarity of the ^{18}F-ArBF$_3^-$ prosthetic group, for which the overall polarity of RGD-trAz-^{18}F-ArBF$_3^-$ was measured in terms of an octanol-water partition, log(P_{OW}), which was found to be -3.8. Nevertheless, there was also substantial uptake in the liver, spleen, and gall bladder immediately following injection. Reasonable tumor-to-muscle ratios (3.88 vs. 8.16 at 30 min. post-injection; 4.08 vs. 7.80 at 60 min. post-injection) [22, 28, 29] were obtained while the RGD-trAz-^{18}F-ArBF$_3^-$ demonstrated slightly better tumor-to-muscle ratio despite of its lower specific activity. Bone uptake appeared to be minimal in both scans and this is consistent with previous reports on the *in vivo* stability of the ^{18}F-ArBF$_3^-$ moiety. Indeed, recent work in our lab (unpublished) has observed signal in the bone at approximately 0.5%-1% ID/g. While this may be due to slow solvolytic defluorination

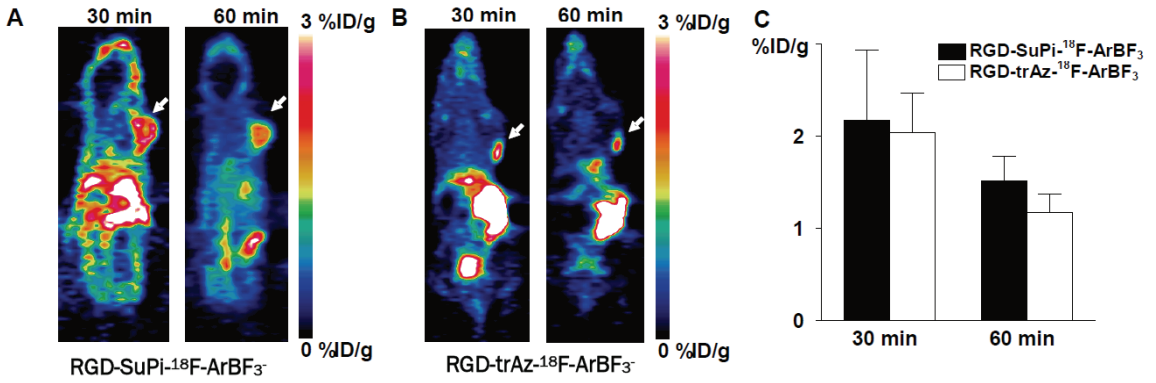

Figure 6. Representative coronal PET images of U87MG tumor bearing mice using RGD-SuPi-^{18}F-ArBF$_3^-$ (A) and RGD-trAz-^{18}F-ArBF$_3^-$ (B). 3.7 MBq of radioactivity was administered via tail vein injection. Five-minute static PET images were acquired at 30 and 60 min. post-injection. Tumors are indicated by arrows. (C) Uptake values at 30 and 60 min. time points in the U87MG tumor quantified from region of interest (ROI) analysis (n = 3).

and/or metabolism of the radiotracer to liberate ^{18}F-fluoride anion, we contend that this level of bone uptake is not inconsistent with other radiotracers.

Because of the widespread acceptance of tumour-specific uptake of labeled RGDs we did not perform a blocking study in this preliminary work. Nevertheless, the lower tumour uptake in the images obtained with RGD-trAz-^{18}F-ArBF$_3^-$, that had been prepared at lower specific activity, serves to demonstrate tumor specificity. Interestingly however, despite the fact that RGD-trAz-^{18}F-ArBF$_3^-$ was prepared at lower specific activity (we used less ^{18}F-fluoride anion to start with), it appeared to have increased specificity for the tumor after 60 minutes. This suggests that linker arm chemistries may play subtle yet important roles in terms of tumor specificity [55].

Notably well-defined tumor images were obtained despite the rather low specific activity of labeling ca. 0.16 Ci/μmol and 0.06 Ci/μmol respectively. It is worth noting that 1 Ci at a specific activity of 2 Ci/μmol would provide 400 nmol total fluoride anion, or approximately the same quantity of total fluoride we used for the labeling. Hence had we used 1-2 Ci, that are commonly available to production labs, the use of added carrier ^{19}F-fluoride could be avoided while specific activities would have increased substantially to >2 Ci/μmol. The ability to generate an ^{18}F-ArBF$_3^-$ at much higher specific activity has been previously discussed [34, 39] and recently we have synthesized an ^{18}F-ArBF$_3^-$ at 15 Ci/μmol (submitted). Work towards higher yields and higher specific activity are underway.

While higher specific activity would likely provide greater contrast, this work was undertaken to validate the use of an ^{18}F-ArBF$_3^-$ in the context of RGD. Moreover, we felt it was important to address the reason for which relatively poor images were obtained with Marimastat. Whereas molecular imaging is a complex phenomenon where all aspects of the radiotracer can affect image quality, here we labeled RGD via very similar radiosynthetic methods at roughly the same specific activity as we obtained for Marimastat. In contrast to poorly defined images with Marimastat, here we obtained quite well defined tumor images suggesting that for ^{18}F-ArBF$_3^-$ bioconjugates, image quality is likely to be dominated by the targeting ligand and not the effect of the pendant ^{18}F-ArBF$_3^-$ moiety. Based on the tumor specific images herein, one may surmise that the hydrophilicity of the ^{18}F-ArBF$_3^-$ appendage that renders the tracer more polar may account for the relatively high tumor specific uptake despite low specific activity. Although in the absence of a blocking experiment we cannot be entirely certain to what extent the ^{18}F-ArBF$_3^-$ moiety contributed to specific tumor uptake, it would be extraordinary if the tumor image were due to specific uptake of the ^{18}F-ArBF$_3^-$ and not the RGD.

Conclusion

For the first time, RGD has been labeled with a prosthetic ^{18}F-ArBF$_3^-$. We featured both direct and indirect labeling that provided reasonable

overall radiochemical chemical yields (10-30%) although somewhat lower yields on the day of functional imaging. In contrast to Marimastat, which has been similarly labeled at relatively low specific activity but which gave mediocre images of cancer-associated matrix metalloprotease activity [34, 49], here we obtained relatively good animal images with two different RGD-^{18}F-ArBF$_3^-$ compositions. Interestingly, RGD-trAz-^{18}F-ArBF$_3^-$, which was labeled in two steps, demonstrated somewhat better tumor-to-muscle ratios. Moreover, the radiosynthesis of RGD-trAz-^{18}F-ArBF$_3^-$ also provided higher isolated radiochemical yield, which attributes to the application of an acid labile protection group 1,8-diaminonaphthalene. Hence, this method should provide a reliable means for radiolabeling biomolecules for PET imaging studies.

Acknowledgements

This work was supported by grant from the Canadian Cancer Society #20071.

Address correspondence to: Dr. David M Perrin, Chemistry Department, UBC, 2036 Main Mall, Vancouver, B.C., V6T-1Z1, Canada. Phone: 604 822 0567; E-mail: dperrin@chem.ubc.ca

References

[1] Hynes RO. Integrins - Versatility, Modulation, and Signaling in Cell-Adhesion. Cell 1992; 69: 11-25.

[2] Hynes RO. Integrins - Versatility, Modulation, and Signaling in Cell-Adhesion. Cell 1992; 69: 11-25.

[3] Haubner R, Finsinger D and Kessler H. Stereoisomeric peptide libraries and peptidomimetics for designing selective inhibitors of the alpha(V)beta(3) integrin for a new cancer therapy. Angew Chem 1997; 36: 1375-1389.

[4] Aumailley M, Gurrath M, Muller G, Calvete J, Timpl R and Kessler H. Arg-Gly-Asp Constrained within Cyclic Pentapeptides - Strong and Selective Inhibitors of Cell-Adhesion to Vitronectin and Laminin Fragment-P1. Febs Lett 1991; 291: 50-54.

[5] Pierschbacher MD and Ruoslahti E. Cell Attachment Activity of Fibronectin Can Be Duplicated by Small Synthetic Fragments of the Molecule. Nature 1984; 309: 30-33.

[6] Pierschbacher MD and Ruoslahti E. Variants of the Cell Recognition Site of Fibronectin That Retain Attachment-Promoting Activity. Proc Natl Acad Sci USA 1984; 81: 5985-5988.

[7] Ruoslahti E and Pierschbacher MD. New Perspectives in Cell-Adhesion - Rgd and Integrins. Science 1987; 238: 491-497.

[8] Albelda SM and Buck CA. Integrins and Other Cell-Adhesion Molecules. Faseb J 1990; 4: 2868-2880.

[9] Humphries MJ. The Molecular-Basis and Specificity of Integrin Ligand Interactions. J Cell Sci 1990; 97: 585-592.

[10] Ruoslahti E. Integrins. J Clin Investig 1991; 87: 1-5.

[11] Haubner R. alpha(v)beta(3)-integrin imaging: a new approach to characterise angiogenesis? Eur J Nucl Med Mol Imaging 2006; 33: S54-S63.

[12] Liu S. Radiolabeled multimeric cyclic RGD peptides as integrin alpha(v)beta(3) targeted radiotracers for tumor imaging. Mol Pharma 2006; 3: 472-487.

[13] Liu S. Radiolabeled Cyclic RGD Peptides as Integrin alpha(v)beta(3)-Targeted Radiotracers: Maximizing Binding Affinity via Bivalency. Bioconjug Chem 2009; 20: 2199-2213.

[14] Cheng Z, Wu Y, Xiong ZM, Gambhir SS and Chen XY. Near-infrared fluorescent RGD peptides for optical imaging of integrin alpha(v) beta 3 expression in living mice. Bioconjug Chem 2005; 16: 1433-1441.

[15] Ye YP, Bloch S, Xu BG and Achilefu S. Design, synthesis, and evaluation of near infrared fluorescent multimeric RGD peptides for targeting tumors. J Med Chem 2006; 49: 2268-2275.

[16] Schottelius M, Laufer B, Kessler H and Wester HJ. Ligands for Mapping alpha(v)beta(3)-Integrin Expression in Vivo. Acc Chem Res 2009; 42: 969-980.

[17] Wu Y, Zhang XZ, Xiong ZM, Cheng Z, Fisher DR, Liu S, Gambhir SS and Chen XY. microPET imaging of glioma integrin alpha(V)beta(3) expression using Cu-64-labeled tetrameric RGD peptide. J Nucl Med 2005; 46: 1707-1718.

[18] Li ZB, Cai WB, Cao QZ, Chen K, Wu ZH, He LN and Chen XY. ^{64}Cu-Labeled "Tetrameric and octameric RGD peptides for small-animal PET of Tumor alpha(v)beta(3) integrin expression. J Nucl Med 2007; 48: 1162-1171.

[19] Li ZB, Chen K and Chen X. Ga-68-labeled multimeric RGD peptides for microPET imaging of integrin alpha(v)beta(3) expression. Eur J Nucl Med Mol Imaging 2008; 35: 1100-1108.

[20] Dijkgraaf I, Rijnders AY, Soede A, Dechesne AC, van Esse GW, Brouwer AJ, Corstens FHM, Boerman OC, Rijkers DTS and Liskamp RMJ. Synthesis of DOTA-conjugated multivalent cyclic-RGD peptide dendrimers via 1,3-dipolar cycloaddition and their biological evaluation: implications for tumor targeting and tumor imaging purposes. Org Biomol Chem 2007; 5: 935-944.

[21] Decristoforo C, Gonzalez IH, Carlsen J, Rupprich M, Huisman M, Virgolini I, Wester HJ and Haubner R. Ga-68- and In-111-labelled DOTA-RGD peptides for imaging of alpha v beta 3 integrin expression. Eur J Nucl Med Mol Imaging 2008; 35: 1507-1515.

[22] Haubner R, Wester HJ, Weber WA, Mang C, Ziegler SI, Goodman SL, Senekowitsch-Schmidtke R, Kessler H and Schwaiger M. Noninvasive imaging of alpha(v)beta(3) integrin expression using F-18-labeled RGD-containing glycopeptide and positron emission tomography. Cancer Res 2001; 61: 1781-1785.

[23] Haubner R, Kuhnast B, Mang C, Weber WA, Kessler H, Wester HJ and Schwaiger M. [F-18] Galacto-RGD: Synthesis, radiolabeling, metabolic stability, and radiation dose estimates. Bioconjug Chem 2004; 15: 61-69.

[24] Ogawa M, Hatano K, Oishi S, Kawasumi Y, Fujii N, Kawaguchi M, Doi R, Imamura M, Yamamoto M, Ajito K, Mukai T, Saji H and Ito K. Direct electrophilic radiofluorination of a cyclic RGD peptide for in vivo alpha(v)beta(3) integrin related tumor imaging. Nucl Med and Biol 2003; 30: 1-9.

[25] Chen XY, Park R, Shahinian AH, Tohme M, Khankaldyyan V, Bozorgzadeh MH, Bading JR, Moats R, Laug WE and Conti PS. F-18-labeled RGD peptide: initial evaluation for imaging brain tumor angiogenesis. Nucl Med and Biol 2004; 31: 179-189.

[26] Olberg DE, Cuthbertson A, Solbakken M, Arukwe JM, Qu H, Kristian A, Bruheim S and Hjelstuen OK. Radiosynthesis and Biodistribution of a Prosthetic Group ((18)F-FENMA) Conjugated to Cyclic RGD Peptides. Bioconjug Chem 2010; 21: 2297-2304.

[27] Battle MR, Goggi JL, Allen L, Barnett J and Morrison MS. Monitoring Tumor Response to Antiangiogenic Sunitinib Therapy with (18)F-Fluciclatide, an (18)F-Labeled alpha(v)beta(3)-Integrin and alpha(v)beta(5)-Integrin Imaging Agent. J Nucl Med 2011; 52: 424-430.

[28] Chen XY, Liu S, Hou YP, Tohme M, Park R, Bading JR and Conti PS. MicroPET imaging of breast cancer alpha(v)-integrin expression with Cu-64-labeled dimeric RGD peptides. Mol Imaging Biol 2004; 6: 350-359.

[29] Beer AJ, Niemeyer M, Carlsen J, Sarbia M, Nahrig J, Watzlowik P, Wester HJ, Harbeck N and Schwaiger M. Patterns of alpha(v)beta(3) expression in primary and metastatic human breast cancer as shown by F-18-galacto-RGD PET. J Nucl Med 2008; 49: 255-259.

[30] Dijkgraaf I, Rijnders AY, Soede A, Dechesne AC, van Esse GW, Brouwer AJ, Corstens FHM, Boerman OC, Rijkers DTS and Liskamp RMJ. Synthesis of DOTA-conjugated multivalent cyclic-RGD peptide dendrimers via 1,3-dipolar cycloaddition and their biological evaluation: implications for tumor targeting and tumor imaging purposes. Org Biomol Chem 2007; 5: 935-944.

[31] Haubner R, Wester HJ, Burkhart F, Senekowitsch-Schmidtke R, Weber W, Goodman SL, Kessler H and Schwaiger M. Glycosylated RGD-containing peptides, tracer for tumor targeting and angiogenesis imaging with improved biokinetics. J Nucl Med 2001; 42: 326-336.

[32] Haubner R, Wester HJ, Reuning U, Senekowitsch-Schmidtke R, Diefenbach B, Kessler H, Stocklin G and Schwaiger M. Radiolabeled alpha(v)beta(3) integrin antagonists: A new class of tracers for tumor targeting. J Nucl Med 1999; 40: 1061-1071.

[33] Liu SL, Liu ZF, Chen K, Yan YJ, Watzlowik P, Wester HJ, Chin FT and Chen XY. (18)F-Labeled Galacto and PEGylated RGD Dimers for PET Imaging of alpha(v)beta(3) Integrin Expression. Mol Imaging Biol 2010; 12: 530-538.

[34] Li Y, Ting R, Harwig CW, Keller UAD, Bellac CL, Lange PF, Inkster JAH, Schaffer P, Adam MJ, Ruth TJ, Overall CM and Perrin DM. Towards kit-like F-18-labeling of marimastat, a noncovalent inhibitor drug for in vivo PET imaging cancer associated matrix metalloproteases. Medchemcomm 2011; 2: 942-949.

[35] Guo N, Lang LX, Li WH, Kiesewetter DO, Gao HK, Niu G, Xie QG and Chen XY. Quantitative Analysis and Comparison Study of F-18 AlF-NOTA-PRGD2, ^{18}F FPPRGD2 and Ga-68 Ga-NOTA-PRGD2 Using a Reference Tissue Model. Plos One 2012; 7.

[36] Lang LX, Li WH, Guo N, Ma Y, Zhu L, Kiesewetter DO, Shen BZ, Niu G and Chen XY. Comparison Study of F-18 FAl-NOTA-PRGD2, F-18 FP-PRGD2, and Ga-68 Ga-NOTA-PRGD2 for PET Imaging of U87MG Tumors in Mice. Bioconjug Chem 2011; 22: 2415-2422.

[37] Amigues E, Schulz J, Szlosek-Pinaud M, Fernandez P, Silvente-Poirot S, Brillouet S, Courbon F and Fouquet E. F-18 Si-RiboRGD: From Design and Synthesis to the Imaging of alpha(v)beta(3) Integrins in Melanoma Tumors. Chempluschem 2012; 77: 345-349.

[38] Ting R, Adam MJ, Ruth TJ and Perrin DM. Arylfluoroborates and alkylfluorosilicates as potential PET imaging agents: high-yielding aqueous biomolecular ^{18}F-labeling. J Am Chem Soc 2005; 127: 13094-13095.

[39] Ting R, Harwig CW, auf dem Keller U, McCormick S, Austin P, Overall CM, Adam MJ, Ruth TJ and Perrin DM. Towards ^{18}F-Labeled Aryltrifluoroborate Radiotracers - In Vivo PET Imaging of Stable Aryltrifluoroborate Clearance in Mice. J Am Chem Soc 2008; 130: 12045-12055.

[40] Ting R, Lo J, Adam MJ, Ruth TJ and Perrin DM. Capturing aqueous (^{18})F -fluoride with an arylboronic ester for PET: Synthesis and aqueous stability of a fluorescent (^{18})F -labeled aryltrifluoroborate. J Fluor Chem 2008; 129: 349-358.

[41] Ting R, Aguilera TA, Crisp JL, Hall DJ, Eckelman WC, Vera DR and Tsien RY. Fast F-18 Labeling of a Near-Infrared Fluorophore Enables Positron Emission Tomography and Optical Imaging of Sentinel Lymph Nodes. Bioconjug Chem 2010; 21: 1811-1819.

[42] Ceccarini G, Flavell RR, Butelman ER, Synan M, Willnow TE, Bar-Dagan M, Goldsmith SJ, Kreek MJ, Kothari P, Vallabhajosula S, Muir TW and Friedman JM. PET Imaging of Leptin Biodistribution and Metabolism in Rodents and Primates. Cell Metab 2009; 10: 148-159.

[43] Wester HJ, Schottelius M, Scheidhauer K, Meisetschlager G, Herz M, Rau FC, Reubi JC and Schwaiger M. PET imaging of somatostatin receptors: design, synthesis and preclinical evaluation of a novel F-18-labelled, carbohydrated analogue of octreotide. Eur J Nucl Med Mol Imaging 2003; 30: 117-122.

[44] Anderson CJ, Dehdashti F, Cutler PD, Schwarz SW, Laforest R, Bass LA, Lewis JS and McCarthy DW. Cu-64-TETA-Octreotide as a PET imaging agent for patients with neuroendocrine tumors. J Nucl Med 2001; 42: 213-221.

[45] Ujula T, Huttunen M, Luoto P, Perkyl H, Simpura I, Wilson I, Bergman M and Roivainen A. Matrix Metalloproteinase 9 Targeting Peptides: Syntheses, ^{68}Ga-labeling, and Preliminary Evaluation in a Rat Melanoma Xenograft Model. Bioconjug Chem 2010; 21: 1612 - 1621.

[46] Banerjee SR, Pullambhatla M, Byun Y, Nimmagadda S, Green G, Fox JJ, Horti A, Mease RC and Pomper MG. 68Ga-Labeled Inhibitors of Prostate-Specific Membrane Antigen (PSMA) for Imaging Prostate Cancer. J Med Chem 2010; 53: 5333–5341.

[47] Chen Y, Foss CA, Byun Y, Nimmagadda S, Pullambahatla M, Fox JJ, Castanares M, Lupold SE, Babich JW, Mease RC and Pomper MG. Radiohalogenated Prostate-Specific Membrane Antigen (PSMA)-Based Ureas as Imaging Agents for Prostate Cancer. J Med Chem 2008; 51: 7933-7943.

[48] Flavell RR, Kothari P, Bar-Dagan M, Synan M, Vallabhajosula S, Friedman JM, Muir TW and Ceccarini G. Site-specific F-18-labeling of the protein hormone leptin using a general two-step ligation procedure. J Am Chem Soc 2008; 130: 9106-9112.

[49] Keller UAD, Bellac CL, Li Y, Lou YM, Lange PF, Ting R, Harwig C, Kappelhoff R, Dedhar S, Adam MJ, Ruth TJ, Benard F, Perrin DM and Overall CM. Novel Matrix Metalloproteinase Inhibitor F-18 Marimastat-Aryltrifluoroborate as a Probe for In vivo Positron Emission Tomography Imaging in Cancer. Cancer Res 2010; 70: 7562-7569.

[50] Thumshirn G, Hersel U, Goodman SL and Kessler H. Multimeric cyclic RGD peptides as potential tools for tumor targeting: Solid-phase peptide synthesis and chemoselective oxime ligation. Chem Eur J 2003; 9: 2717-2725.

[51] Thumshirn G, Hersel U, Poethko T, Rau F, Haubner R, Schwaiger M, Wester HJ and Kessler H. Multimeric cyclic RGD peptides with improved tumor uptake for tumor targeting. Peptide Revolution: Genomics, Proteomics & Therapeutics 2004; 693-694.

[52] Liu ZF, Liu SL, Wang F, Liu S and Chen XY. Noninvasive imaging of tumor integrin expression using (^{18})F-labeled RGD dimer peptide with PEG(4) linkers. Eur J Nucl Med Mol Imaging 2009; 36: 1296-1307.

[53] Auzzas L, Zanardi F, Battistini L, Burreddu P, Carta P, Rassu G, Curti C and Casiraghi G. Targeting alpha(v)beta(3) Integrin: Design and Applications of Mono- and Multifunctional RGD-Based Peptides and Semipeptides. Curr Med Chem 2010; 17: 1255-1299.

[54] Dechantsreiter MA, Planker E, Matha B, Lohof E, Holzemann G, Jonczyk A, Goodman SL and Kessler H. N-methylated cyclic RGD peptides as highly active and selective alpha(v)beta(3) integrin antagonists. J Med Chem 1999; 42: 3033-3040.

[55] Kolb HC and Sharpless KB. The growing impact of click chemistry on drug discovery. Drug Discov Today 2003; 8: 1128-1137.

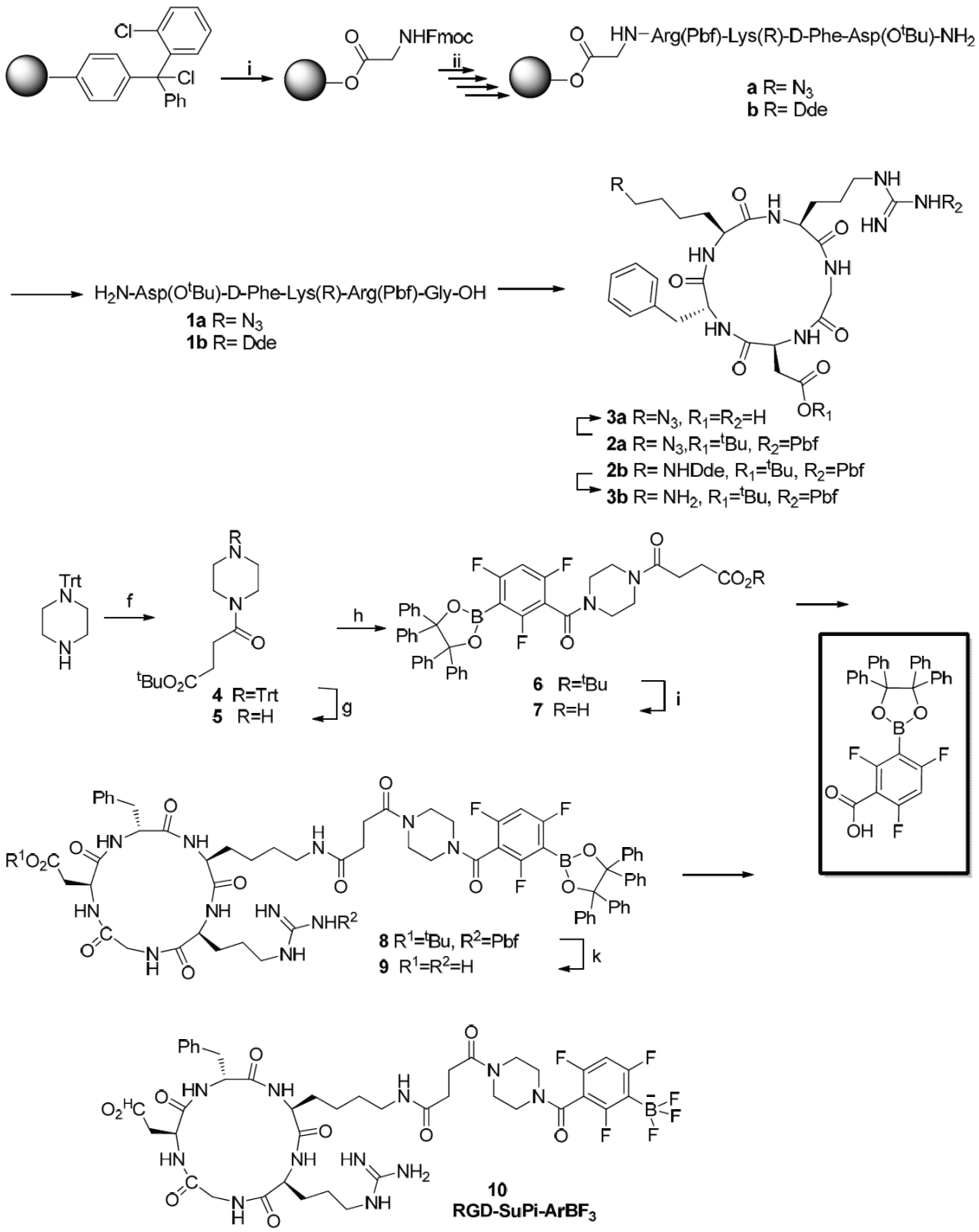

Peptide syntheses: In general, the linear precursors of the RGD peptides, where the lysine ε-amino group was either protected with the Dde group or first converted to the azide, were prepared via solid phase peptide synthesis. Linear peptides were then cyclized to provide the cyclo-RGD whereupon the lysine residue was further acylated with boronate.

H-Asp(O^{t}Bu)-*D*-Phe-Lys(R)-Arg(Pbf)-Gly-OH (1a/b): The linear peptide was prepared following the standard Fmoc solid phase peptide synthesis with 2-chlorotrityl chloride resin. [59, 60] Briefly, Fmoc-Gly-OH (1.00 g, 3.38 mmol) and DIPEA (2.35 mL, 13.52 mmol) were suspended in anhydrous CH_2Cl_2 (20 mL) in

a flame-dried round bottom flask under an Ar atmosphere. DMF (6 mL) was added to assist to dissolve the amino acid prior to the addition of the 2-Cl-trityl chloride resin (2.00 g, 2.60 mmol). The mixture was stirred at room temperature for 90 min. and the solution was filtered. The capping solution (MeOH:DIPEA:CH_2Cl_2 2:1:17, 3 × 20 mL) was mixed thoroughly with the resin and slowly filtered off by gravity. Then the resin was washed with CH_2Cl_2 (3 × 20 mL), DMF (3 × 20 mL), and CH_2Cl_2 (6 × 20 mL), and dried thoroughly over high vacuum. The Fmoc-Gly-attached resin was directly used without further treatment. The resin loading of the Fmoc-Gly-resin was tested based on the DBU/DMF/CH_3CN method and the reported extinction coefficient (7624 M^{-1}·cm^{-1}) for 9-methylene-*9H*-fluorene at 304 nm was used. Then the resin was swollen in DMF (1.5 volumes of the resin) for 30 min. prior to the synthesis in a spin column (5 mL or 10 mL) sealed with a plastic pipette tip. The DMF was filtered and Fmoc was removed with 20% piperidine/DMF (1.5 volumes of the resin) 3 times with each time for 5 min.. Then the resin was thoroughly washed with DMF (3 × 10 mL), CH_2Cl_2 (3 × 10 mL), and DMF (3 × 10 mL). Fmoc-Arg(Pbf)-OH (4 equivalents) and HBTU (4 equivalents) in DMF (1.5 volumes of the resin) was added to the resin followed by the addition of DIPEA (8 equivalents). The spin column was capped and shaken at room temperature for 2 hr. Then the solution was directly filtered through the spin column and the resin was washed with DMF (3 × 10 mL), CH_2Cl_2 (3 × 10 mL), and DMF (3 × 10 mL) before the next cycle of the addition of the next amino acid (Fmoc-Lys(R)-OH, Fmoc-*D*-Phe-OH, and the last Fmoc-Asp(O^{t}Bu)-OH). After the fifth amino acid (Fmoc-Asp(O^{t}Bu)-OH) was attached, the Fmoc group was removed following the same procedure and the resin was thoroughly washed with DMF (3 × 10 mL), CH_2Cl_2 (3 × 10 mL), DMF (3 × 10 mL), and CH_2Cl_2 (5 × 10 mL), and dried over vacuum to remove the residual solvent. Then the resin was transferred to a round bottom flask and treated with 20% HFIP/CH_2Cl_2 (10 volumes of the resin). The mixture was incubated at room temperature for 20 min. and then filtered off. The filtrate was concentrated under reduced pressure and the residue was triturated with MeOH/Et_2O to give a whitish solid. The peptides were used for cyclization without further purification. Peptides **1a**/**b** were analyzed with RP-HPLC in Agilent 1100 series with Column I, using HPLC Program 1: gradient: solvent A: 0.1% TFA in H_2O, solvent B: 0.05% TFA in CH_3CN, 0 min. to 2 min., 10% B, 2 min. to 20 min., 10% B to 50% B, 20 min. to 25 min., 50% B to 100% B, 25 min. to 28 min., 100% B, 28 min. to 30 min., 100% B to 10% B, 30 min. to 32 min., 10% B, column temperature 50 °C, flow rate: 1 mL/min. The desired peptide was characterized with ESI mass spectrometry. H-Asp(O^{t}Bu)-*D*-Phe-Lys(N_3)-Arg(Pbf)-Gly-OH **1a** t_R = 25.4 min.; ESI-HRMS: calcd. for $C_{44}H_{66}N_{11}O_{11}S^+$: 956.4664, found: 956.4639; H-Asp(O^{t}Bu)-*D*-Phe-Lys(Dde)-Arg(Pbf)-Gly-OH **1b** t_R = 25.2 min.; ESI-HRMS: calcd. for $C_{54}H_{80}N_9O_{13}S^+$: 1094.5596, found: 1094.5588.

***Cyclo*[Arg(Pbf)-Gly-Asp(O^{t}Bu)-*D*-Phe-Lys(N_3)] (2a):** The linear peptide H-Asp(O^{t}Bu)-*D*-Phe-Lys(N_3)-Arg(Pbf)-Gly-OH **1a** (100 mg, 0.105 mmol) and DIPEA (54.7 µL, 0.314 mmol) in CH_3CN (105 mL) was added with HBTU (119 mg, 0.314 mmol). The resulting mixture was stirred at room temperature for 24 hr and concentrated under reduced pressure. Then the residue was suspended in EtOAc (100 mL) and H_2O (100 mL) was added to wash the EtOAc layer. The aqueous layer was further extracted with EtOAc (2 × 100 mL). The organic layers were combined, washed with brine (2 × 100 mL), and dried over anhydrous Na_2SO_4. The solution was filtered and concentrated to give colorless oil. The residue was then dissolved in minimum MeOH (~ 5 mL) and Et_2O (300 mL) was added to precipitate the peptide. The solid was filtered off, washed thoroughly with Et_2O, dried over high vacuum, and used directly without further purification. Yield: 74.5 mg, 76%. The quality of the peptide was determined by RP-HPLC with HPLC Program 1 and Column I in Agilent 1100 series, t_R = 26.2 min.. ^{1}H NMR (400 MHz, d_4-MeOD, rt): δ(*ppm*) 1.06 (m, 2 H), 1.45 (m, 20 H), 1.68 (m, 2 H), 1.84 (m, 1 H), 2.09 (s, 3 H), 2.51 (m, 4 H), 2.57 (s, 3 H), 2.75 (m, 1 H), 2.98 (m, 1 H), 3.02 (s, 3 H), 3.20 (m, 4 H), 3.99 (m, 1 H), 4.23 (m, 2 H), 4.55 (m, 1 H), 4.75 (m, 1 H), 7.21-7.32 (m, 5 H), 7.90 (m, 1 H), 8.21 (m, 1 H), 8.42 (m, 1 H); ESI-HRMS: calcd. for $C_{44}H_{64}N_{11}O_{10}S^+$: 938.4558, found: 938.4542.

***Cyclo*[Arg(Pbf)-Gly-Asp(O^{t}Bu)-*D*-Phe-Lys(Dde)] (2b):** The linear peptide H-Asp(O^{t}Bu)-*D*-Phe-Lys(Dde)-Arg(Pbf)-Gly-OH **1b** (200 mg, 0.182 mmol) and DIPEA (96 µL, 0.549 mmol) in CH_3CN (200 mL) was added with HBTU (208 mg, 0.182 mmol). The resulting mixture was stirred at room temperature for 24 hr and then concentrated under reduced pressure. The residue was suspended in EtOAc (100 mL) and H_2O (100 mL) was added to wash the EtOAc layer. The aqueous layer was further extracted with EtOAc (2 × 100 mL). The organic layers were combined, washed with brine (2 × 100 mL), and dried over anhydrous Na_2SO_4. The solution was filtered and concentrated to give colorless oil. The residue was then

dissolved in minimum MeOH (~ 5 mL) and Et_2O (300 mL) was added to precipitate the peptide. The solid was filtered off, washed thoroughly with Et_2O, dried over vacuum, and used directly without further purification. Yield: 184.3 mg, 94%. The quality of the peptide was determined by RP-HPLC with HPLC Program 1 and Column I in Agilent 1100 series, t_R = 26.0 min.. ESI-HRMS: calcd. for $C_{54}H_{77}N_9O_{12}NaS^+$: 1098.5310, found: 1098.5328.

***Cyclo*[Arg-Gly-Asp-*D*-Phe-Lys(N_3)] (*c*[RGDfK(N_3)]) (3a):** The protected peptide **2a** *cyclo*[Arg(Pbf)-Gly-Asp-*D*-Phe-Lys(N_3)] (74.5 mg, 0.0794 mmol) was dissolved in TFA:H_2O (20:1, 42 mL) and the reaction was stirred at room temperature for 3 hr. Then the solution was concentrated under reduced pressure and toluene (3 × 20 mL) was added to the residue to azeotropically remove the residual TFA and H_2O. The residue was then dissolved in a minimal amount of MeOH (~ 2 mL) and triturated with Et_2O (~ 30 mL) resulting in a white solid. The mixture was filtered. The solid was washed with Et_2O thoroughly and dried over vacuum. Yield: 45.0 mg, 90%. The crude peptide was further purified via semi-preparative HPLC via HPLC Program 2 (gradient: solvent A: 0.1% TFA in water, solvent B: 0.05% TFA in CH_3CN, 0 min. to 1 min., 5% B to 10% B, 1 min. to 10 min., 10% B to 50% B, 10 min. to 13 min., 50% B to 100% B, 13 min. to 14 min., 100% B; column temperature: 50°C; flow rate: 3 mL/min.) with Column II in Agilent 1100 series, t_R = 10.9 min. or analyzed via HPLC Program 1 with Column I in Agilent 1100 series, t_R = 15.1 min.. ^{1}H NMR (400 MHz, d_6-DMSO, rt): δ (*ppm*) 1.06 (m, 2 H), 1.27-1.53 (m, 6 H), 1.54 (m, 1 H), 1.71 (m, 1 H), 2.36 (dd, J_1 = 16.24 Hz, J_2 = 5.60 Hz, 1 H), 2.69 (dd, J_1 = 16.26 Hz, J_2 = 8.70 Hz, 1 H), 2.79 (m, 1 H), 2.91 (m, 1 H), 3.06 (m, 2 H), 3.22 (m, 3 H), 3.93 (m, 1 H), 4.03 (dd, J_1 = 14.18 Hz, J_2 = 7.82 Hz, 1 H), 4.13 (dd, J_1 = 14.14 Hz, J_2 = 7.22 Hz, 1 H), 4.43 (dd, J_1 = 14.16 Hz, J_2 = 7.24 Hz, 1 H), 4.62 (m, 1 H), 6.87 (s, br, 2 H), 7.10-7.29 (m, 7 H), 7.57 (t, *J* = 5.48 Hz, 1 H), 7.69 (d, *J* = 3.92 Hz, 1 H), 8.00-8.16 (m, 3 H), 8.40 (m, 1 H); ^{13}C NMR (100.6 MHz, d_6-DMSO, rt): δ (*ppm*) 23.29, 25.81, 28.18, 28.97, 31.38, 35.66, 37.87, 43.81, 49.48, 51.00, 52.51, 54.92, 126.87, 128.71, 129.70, 137.89, 157.25, 170.11, 170.57, 171.18, 171.70, 172.26, 172.61; ESI-HRMS: calcd. for $C_{27}H_{40}N_{11}O_7^+$: 630.3122, found: 630.3119.

***Cyclo*[Arg(Pbf)-Gly-Asp(O^{t}Bu)-*D*-Phe-Lys] (3b):** The peptide *cyclo*[Arg(Pbf)-Gly-Asp(O^{t}Bu)-*D*-Phe-Lys(Dde)] **2b** (106 mg, 0.099 mmol) in THF (10 mL) was added with $NH_2NH_2{\cdot}H_2O$ (0.4 mL). The resulting mixture was stirred at room temperature for 20 min. and the solution was concentrated under reduced pressure. The residue was dissolved in a minimal volume of MeOH (~ 1.5 mL) and Et_2O (40 mL) was added to precipitate the peptide. The peptide was filtered off, washed with Et_2O, dried over high vacuum, and then used directly in the following step without further purification. Yield: 78.4 mg, 87%. The quality of the peptide was determined by RP-HPLC with HPLC Program 1 and Column I in Agilent 1100 series, t_R = 22.3 min.. ESI-HRMS: calcd. for $C_{44}H_{66}N_9O_{10}S^+$: 912.4653, found: 912.4633.

***N*-Tritylpiperazine:** Trityl chloride (2.0 g, 7.0 mmol) was added in one portion to piperazine (3.0 g, 34.8 mmol) in CH_2Cl_2 (20.0 mL) at 0°C. Then the ice-water bath was removed and the reaction was stirred at room temperature for 0.5 hr. The reaction was then quenched by the addition of H_2O (50 mL) and extracted with CH_2Cl_2 (3 × 50 mL). The CH_2Cl_2 layers were combined, washed with H_2O (2 × 50 mL) and brine (1 × 50 mL), and dried over anhydrous Na_2SO_4. The solution was then filtered and concentrated under reduced pressure. The residue was treated with flash chromatography (MeOH: CH_2Cl_2 3:97) to afford a white solid as the desired product (R_f = 0.53 in 1:9 MeOH: CH_2Cl_2). Yield: 1.48 g, 64%. ^{1}H NMR (300 MHz, CD_2Cl_2, rt): δ(*ppm*) 2.15 (s, 2 H), 2.99 (s, 6 H), 7.18 (m, 3 H), 7.29 (d, *J* = 7.73 Hz, 6 H), 7.48 (s, 6 H); ^{13}C NMR (100.6 MHz, CD_2Cl_2, rt): δ(*ppm*) 46.82, 49.87, 77.45, 126.07, 127.55, 129.55.

Mono-*tert*-butyl succinate: Succinic anhydride (3.0 g, 30.0 mmol), *N*-hydroxyl succinimide (1.0 g, 8.7 mmol), DMAP (0.35 g, 2.9 mmol), and NEt_3 (1.25 mL, 9.0 mmol) were dissolved in ^{t}BuOH (5.0 mL) and toluene (50.0 mL). The reaction was heated to reflux for 24 hr. Once cooled to room temperature, the reaction was diluted with EtOAc (50 mL) and washed with 10% aqueous citric acid solution (50 mL). The layers were separated and the aqueous layer was further extracted with EtOAc (2 × 50 mL). The combined organic layers were washed with 10% aqueous citric acid (2 × 50 mL) and brine (1 × 50 mL), and dried over anhydrous Na_2SO_4. The solution was then filtered and concentrated under reduced pressure. The residue was purified by flash chromatography (1:3 EtOAc: hexanes, visualized on TLC by *p*-anisaldehyde stain) to give a white solid as the product (R_f = 0.16 in 1:1 EtOAc:hexanes). Yield: 2.45 g, 47%. ^{1}H NMR (300 MHz, $CDCl_3$, rt): δ(*ppm*) 1.46 (d, *J*= 1.69 Hz, 9 H), 2.54 (m, 2 H), 2.64 (m, 2 H); ^{13}C NMR (75.5 MHz, $CDCl_3$, rt): δ(*ppm*) 28.16, 29.33, 30.23, 81.16, 171.54, 178.81; ESI-LRMS: $[M+Na]^+$, 197.1 (100%).

***Tert*-butyl 4-oxo-4-(4-tritylpiperazin-1-yl)butanoate (4):** HBTU (493 mg, 1.30 mmol) was added to *N*-tritylpiperazine (330 mg, 1.00 mmol), *tert*-butyl succinate (200 mg, 1.15 mmol), and NEt_3 (0.42 mL, 3.0 mmol) in CH_2Cl_2 (10.0 mL). The reaction was undertaken at room temperature for 2.5 hr. To the reaction was added 10% aqueous citric acid solution (30 mL) and extracted with CH_2Cl_2 (3 × 50 mL). The organic layers were combined and washed with H_2O (1 × 50 mL), saturated $NaHCO_3$ (1 × 50 mL), H_2O (1 × 50 mL), and brine (1 × 50 mL). After drying over anhydrous Na_2SO_4, the CH_2Cl_2 solution was concentrated under vacuum. The residue was resuspended in a minimal volume of EtOAc and the product was purified by silica gel flash chromatography (EtOAc:hexanes 1:9 then 1:6) to give a white solid as the desired product (R_f = 0.51 in 1:1 EtOAc:hexanes). Yield: 473.8 mg, 98%. ^{1}H NMR (400 MHz, CD_2Cl_2, rt): δ(*ppm*) 1.40 (s, 9 H), 2.28 (s, br, 2 H), 2.45 (s, 4 H), 3.61 (m, 2 H), 3.72 (s, br, 2 H), 7.21 (m, 3 H), 7.31 (m, 6 H), 7.51 (m, 6 H); ^{13}C NMR (100.6 MHz, CD_2Cl_2, rt): δ(*ppm*) 27.90, 30.50, 42.15, 45.81, 47.98, 48.40, 77.15, 80.07, 126.35, 127.75, 129.40, 169.77, 172.25.

***Tert*-butyl 4-oxo-4-(piperazin-1-yl)butanoate (5):** *Tert*-butyl ester **4** (110.0 mg, 0.227 mmol) and HFIP (1.2 mL, 11.4 mmol) were dissolved in trifluoroethanol (5.0 mL) and stirred at 40°C for 4 hr. The reaction was concentrated *in vacuo* to give oily residue. The residue was then resuspended in a minimal volume of EtOAc and the product was purified by silica flash chromatography (MeOH:CH_2Cl_2 3:97 then 1:9) and colorless oil was obtained as the desired product (R_f = 0.13 in 1:9 MeOH:CH_2Cl_2). Yield: 52.9 mg, 96%. ^{1}H NMR (400 MHz, $CDCl_3$, rt): δ(*ppm*) 1.46 (d, *J* = 1.35 Hz, 9 H), 2.58 (d, *J* = 1.11 Hz, 4 H), 2.90 (d, *J* = 15.88 Hz, 4 H), 3.17 (s, br, 2 H), 3.52 (s, 2 H), 3.63 (s, 2 H); ^{13}C NMR (100.6 MHz, $CDCl_3$, rt): δ(*ppm*) 28.32, 28.52, 30.85, 42.78, 45.18, 45.91, 46.27, 80.89, 170.34, 172.79; ESI-LRMS: $[M+Na]^+$, 265.1 (100%).

***Tert*-butyl 4-oxo-4-(4-(2,4,6-trifluoro-3-(4,4,5,5-tetraphenyl-1,3,2-dioxaborolan-2-yl) benzoyl)piperazin-1-yl)butanoate (6):** *Tert*-butyl ester **5** (91.1 mg, 0.376 mmol), the tetraphenylpinacolate of 2,4,5-trifluoro-3-carboxy-phenyl-1-boronic acid (238.0 mg, 0.432 mmol), HOBt·H_2O (73.0 mg, 0.475 mmol), and pyridine (0.14 mL, 1.79 mmol) were dissolved in CH_2Cl_2 (15 mL) and added with EDC·HCl (125.0 mg, 0.648 mmol) in one portion. The resulting mixture was reacted at room temperature overnight and then quenched by the addition of 10% aqueous citric acid solution (50 mL). The product was extracted into CH_2Cl_2 (3 × 50 mL). The organic layers were combined, washed with H_2O (1 × 50 mL) and brine (1 × 50 mL), and dried over anhydrous Na_2SO_4. The solution was filtered and the solvent was removed under vacuum. The residue was isolated via silica gel flash chromatography (MeOH:CH_2Cl_2 0:100 to 1:99) to afford a white solid as the desired product (R_f = 0.63 in 1:9 MeOH:CH_2Cl_2). Yield: 241.0 mg, 83%. ^{19}F NMR (282.4 MHz, CD_2Cl_2, rt): δ(*ppm*) -28.75 (s, 1 F), -22.36 (s, 1 F), -17.25 (s, 1 F); ^{1}H NMR (400 MHz, CD_2Cl_2, rt): δ(*ppm*) 1.45 (s, 9 H), 2.58 (m, 4 H), 3.41-3.85 (m, 8 H), 6.91 (t, *J* = 8.80 Hz, 1 H), 7.13 (m, 12 H), 7.21 (m, 4 H), 7.26 (t, *J* = 3.54 Hz, 4 H); ^{13}C NMR (100.6 MHz, CD_2Cl_2, rt): δ(*ppm*) 27.93, 28.00, 30.45, 42.06, 46.80, 80.31, 96.98, 101.26, 127.26, 127.32, 127.45, 128.62, 128.65, 141.82, 142.17, 170.18, 172.12; ESI-HRMS: calcd. for $C_{45}H_{43}BN_2O_6F_3^+$: 775.3166, found: 775.3174.

4-Oxo-4-(4-(2,4,6-trifluoro-3-(4,4,5,5-tetraphenyl-1,3,2-dioxaborolan-2-yl)benzoyl) piperazin-1-yl)butanoic acid (7): TFA (5.0 mL) was added to *tert*-butyl ester **6** (77.3 mg, 0.0998 mmol) in CH_2Cl_2 (10.0 mL) and the mixture was stirred at room temperature for 3 hr. The mixture was then concentrated under vacuum and the residue was purified via silica gel flash chromatography (MeOH:CH_2Cl_2 1:200 to 1:99) to afford white foam as the desired product (R_f = 0.32 in 1:9 MeOH:CH_2Cl_2). Yield: 62.9 mg, 88%. ^{19}F NMR (282.4 MHz, CD_2Cl_2, rt): δ(*ppm*) -28.84 (s, 1 F), -22.47 (s, 1 F), -16.99 (s, 1 F); ^{1}H NMR (400 MHz, CD_2Cl_2, rt): δ(*ppm*) 2.70 (m, 4 H), 3.41-3.89 (m, 8 H), 6.75 (s, br, 1 H), 6.91 (t, *J* = 8.91 Hz, 1 H), 7.08-7.27 (m, 20 H); ^{13}C NMR (100.6 MHz, CD_2Cl_2, rt): δ(*ppm*) 28.07, 29.45, 41.61, 42.00, 42.21, 45.18, 45.71, 97.00, 101.33, 127.28, 127.33, 127.45, 128.62, 128.64, 141.74, 141.82, 142.13, 159.71, 171.03, 175.67; ESI-HRMS: calcd. for $C_{41}H_{34}BN_2O_6F_3Na^+$: 741.2360, found: 741.2346.

***Cyclo*[Arg(pbf)-Gly-Asp(O^{t}Bu)-*D*-Phe-Lys(suc-piperazinyl-boronate)] (8):** EDC·HCl (16.0 mg, 57.5 μmol) was added to the DMF solution (1.5 mL) of **7** (27.7 mg, 38.6 μmol), *cyclo*[Arg(Pbf)-Gly-Asp(O^{t}Bu)-*D*-Phe-Lys] **3b** (23.0 mg, 25.5 μmol), HOBt·H_2O (7.0 mg, 57.5 μmol), and pyridine (24.0 μL, 0.27 mmol). The DMF solution was stirred at room temperature for 36 hr. The reaction mixture was then quenched with 10% aqueous citric acid (20 mL) and extracted with EtOAc (3 × 30 mL). The EtOAc layers were combined,

washed with H_2O (1 × 30 mL) and brine (1 × 30 mL), and dried over anhydrous Na_2SO_4. The solution was filtered and concentrated under reduced pressure, and the residue was dissolved in a minimal volume of MeOH (~ 1 mL). Et_2O (20 mL) was added to the methanolic solution to precipitate the peptide. The mixture was filtered and the pellet was washed with Et_2O thoroughly to give a whitish solid, which was directly used in the following step without further purification. Yield: 31.7 mg, 77%. The quality of the peptide was determined by RP-HPLC with HPLC Program 1 and Column I in Agilent 1100 series, t_R = 28.2 min.. ESI-HRMS: calcd. for $C_{85}H_{98}BN_{11}O_{15}F_3S^+$: 1612.7010, found: 1612.6984.

***Cyclo*[Arg-Gly-Asp-*D*-Phe-Lys(suc-piperazinyl-boronate)] (9):** The protected peptide **8** (31.7 mg, 0.0197 mmol) was dissolved in TFA (12 mL) and H_2O (0.58 mL). The reaction was incubated at room temperature for 1.5 hr and the solvent was removed under vacuum. The residue was then dissolved in a minimal volume of MeOH (~ 2 mL) whereupon Et_2O (30 mL) was added to precipitate the peptide. The mixture was filtered and the pellet was thoroughly washed with Et_2O to give a whitish powder as the crude product. Yield: 21.1 mg, 82%. The product was analyzed by RP-HPLC via HPLC Program 1 and Column I in Agilent 1100 series, t_R = 26.2 min. The crude peptide (~ 10 mg) was dissolved in CH_3CN containing 10% H_2O (2 mL) and purified by semi-preparative HPLC via HPLC Program 3 (gradient: solvent A: 0.1% TFA in water, solvent B: 0.05% TFA in CH_3CN, 0 min. to 1 min., 20% B to 30% B, 1 min. to 3 min., 30% B to 50% B, 3 min. to 10 min., 50% B to 100% B, 10 min. to 13 min., 100% B, 13 min. to 15 min., 100% B to 50% B, 15 min. to 16 min., 50% B to 20% B; column temperature: 50°C; flow rate: 3 mL/min) and Column II in Agilent 1100 series (t_R = 9.7 min) to give a white solid. Yield: 4.0 mg, 47%. ^{19}F NMR (282.4 MHz, MeOD, rt): δ(*ppm*) -29.73 (s, 1 F), -23.76 (s, 1 F), -17.35 (s, 1 F); ^{1}H NMR (400 MHz, MeOD, rt): δ(*ppm*) 1.04 (m, 2 H), 1.31 (s, 1 H), 1.40-1.47 (m, 3 H), 1.54 (m, 2 H), 1.67 (m, 2H), 1.87 (m, 1 H), 2.34 (s, 2 H), 2.46-2.62 (m, 3 H), 2.64-2.90 (m, 3 H), 2.99 (m, 2 H), 3.03-3.19 (m, 3 H), 3.49 (m, 2 H), 3.55 (m, 1 H), 3.58-3.69 (m, 3 H), 3.72 (m, 2 H), 3.81 (m, 1 H), 3.89 (m, 1 H), 3.94 (m, 1 H), 4.26 (m, 2 H), 4.55 (m, 1 H), 4.76 (m, 1 H), 7.10 (m, 11 H), 7.14-7.31 (m, 15 H), 7.86 (m, 1 H), 8.23 (m, 1 H), 8.43 (m, 1 H). ESI-HRMS: calcd. for $C_{68}H_{74}BN_{11}O_{12}F_3^+$: 1304.5564, found: 1304.5536.

***Cyclo*[Arg-Gly-Asp-*D*-Phe-Lys(suc-piperazinyl-ArBF$_3^-$)] (10, also referred to RGD-SuPi-ArBF$_3^-$):** The crude peptide **9** (~ 8 mg, 4.96 μmol) was dissolved in MeOH (1 mL) to which was added 4 M KHF_2 (200 μL, 0.80 mmol) in a 15 mL Falcon tube. The reaction was then stirred at room temperature overnight and the solvent was removed under vacuum. Et_2O (10 mL) was added to the residue and the mixture was centrifuged after being thoroughly mixed. The Et_2O layer was discarded. The Et_2O wash was then repeated two more times. The residue was then dried over vacuum to remove the residual Et_2O for 5 hr. Then d_6-DMSO (~ 400 μL) was added to extract the product from the crude. ^{19}F NMR (282.4 MHz, d_6-DMSO, rt): δ(*ppm*) -21.13 (s, 1 F), -27.30 (s, 1 F), -40.54 (s, 1 F), -54.91 (s, 3 F). ESI-LRMS: $[M]^-$, 996.4 (100%).

2,4,6-Trifluoro-3-(*1H*-naphtho[1,8-de][1,3,2]diazaborinin-2(*3H*)-yl)benzoic acid (11): 2,4,6-Trifluorobenzoic acid (0.50 g, 2.8 mmol) was dissolved in anhydrous THF (30 mL) and cooled to -78°C under Ar. 1.6 M BuLi in hexanes (4.0 mL, 6.4 mmol) was slowly added to the solution at the same temperature and the resulting mixture was stirred for 10 min. Then $B(OCH_3)_3$ was added in one portion to the mixture and the reaction was incubated at -78°C for another 3 hr. The reaction was quenched by addition of 4 M HCl in dioxane (2.5 mL, 10 mmol). The reaction was continued to stir at -78°C for 0.5 hr and allowed to warm up to room temperature. The reaction crude was then concentrated under vacuum and 1,8-diaminonaphthalene (0.50 g, 3.0 mmol) in THF (30 mL) and toluene (30 mL) was added to the residue. The mixture was then refluxed overnight and concentrated under vacuum. The product was further purified by flash chromatography (0.5% MeOH in CH_2Cl_2 to 10% MeOH in CH_2Cl_2) to yield grey powder as the desired product. Yield: 0.90 g, 94%. ESI-MS: $[M+H]^+$: 343.0; ^{19}F NMR (282.4 MHz, d_4-MeOD, rt): d (*ppm*) -33.84 (s, 1 Ar-F), -26.51 (s, 1 Ar-F), -23.78 (s, 1 Ar-F); ^{1}H NMR (400 MHz, d_4-MeOD, rt): d (*ppm*) 6.42 (dd, J_1= 9.94 Hz, J_2= .85 Hz, 2 H), 6.83 (td, J_1= 8.14 Hz, J_2= 1.54 Hz, 1 H), 6.94 (dd, J_1= 8.29 Hz, J_2= 0.79 Hz, 2 H)), 7.05 (t, J= 7.81 Hz, 2 H); ^{13}C NMR (400 MHz, d_4-MeOD, rt): d (*ppm*) 99.40, 99.70, 99.97, 105.49, 116.99, 120.32, 127.25, 136.57, 141.69.

Alkyneborimidine (12): 2,4,6-Trifluoro-3-(*1H*-naphtho[1,8-de][1,3,2]diazaborinin-2(*3H*)-yl)benzoic acid (0.17 g, 0.50 mmol), propargylamine (35 μL, 0.55 mmol), HOBt·H_2O (0.10 g, 0.65 mmol), and pyridine (0.65 mL, 8.0 mmol) in DMF (10 mL) was added with EDC·HCl (0.15 g, 0.80 mmol). The resulting mixture

was stirred at room temperature overnight and then concentrated under vacuum. The residue was purified via flash chromatography (10% EtOA in hexanes to 20% EtOAc in hexanes) to give pale green solid. Yield: 93 mg, 49%. ESI-MS: $[M+H]^+$: 380.3; ^{19}F NMR (282.4 MHz, *d*-$CDCl_3$, rt): d (*ppm*) -29.33 (s, 1 Ar-F), -24.98 (s, 1 Ar-F), -19.62 (s, 1 Ar-F); ^{1}H NMR (300 MHz, *d*-$CDCl_3$, rt): d (*ppm*) 2.35 (s, 1 H), 4.31 (*dd*, J_1= 4.91 Hz, J_2= 2.44 Hz, 2 H), 6.14 (s, br, 1 H), 6.40 (*d*, *J*= 7.10 Hz, 2 H), 6.81 (*d*, *J*= 12.0 Hz, 1 H), 7.10 (*m*, 4 H).

NMR spectra

H-Asp(O^{t}Bu)-*D*-Phe-Lys(Dde)-Arg(Pbf)-Gly-OH (1b)

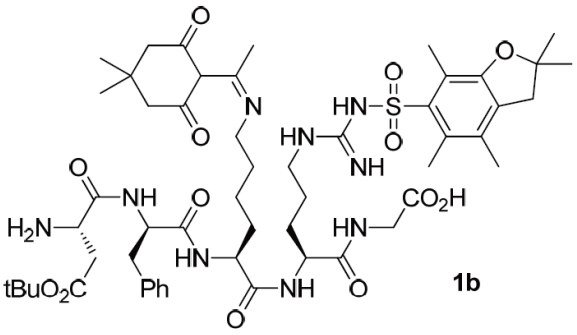

Chemical Formula: $C_{54}H_{79}N_9O_{13}S$
Exact Mass: 1093.5518
Molecular Weight: 1094.3226

^{1}H NMR 400 MHz, ^{1}H-^{1}H-COSY, d_4-MeOD

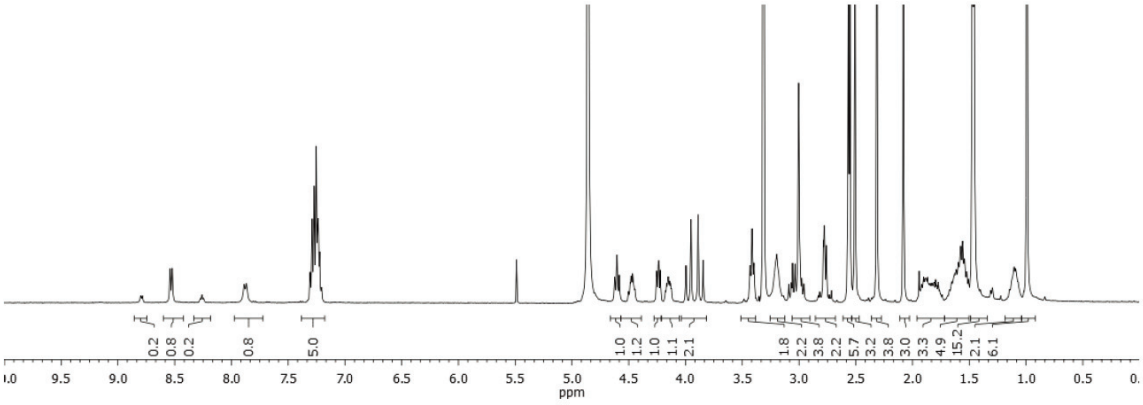

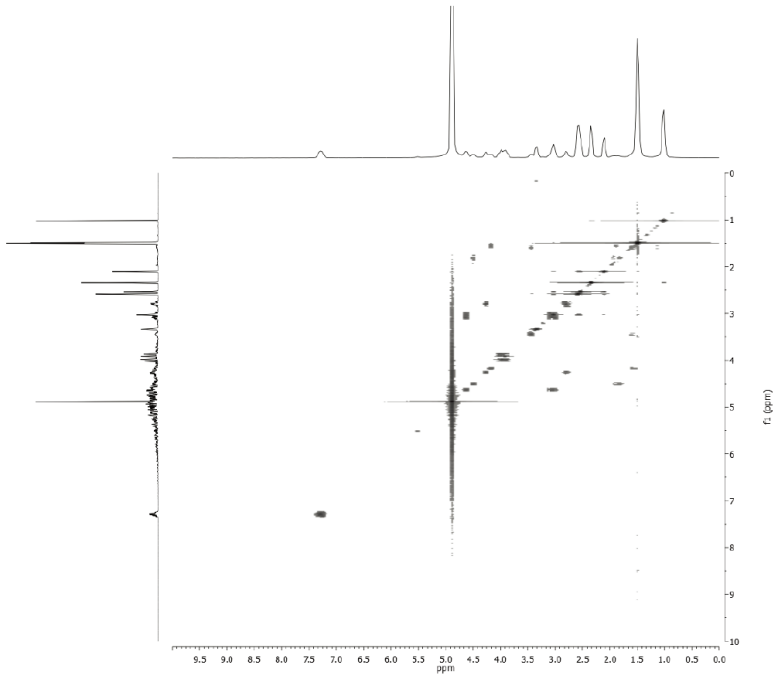

***Cyclo*[Arg(Pbf)-Gly-Asp(O^{t}Bu)-*D*-Phe-Lys(N_3)] (2a)**

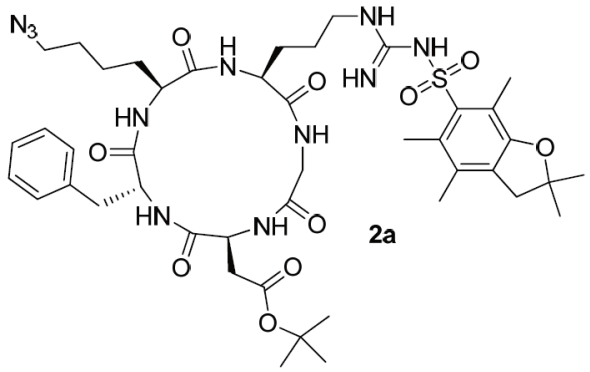

Chemical Formula: $C_{44}H_{63}N_{11}O_{10}S$
Exact Mass: 937.4480
Molecular Weight: 938.1037

^{1}H NMR 400 MHz, ^{1}H-^{1}H-COSY, d_4-MeOD

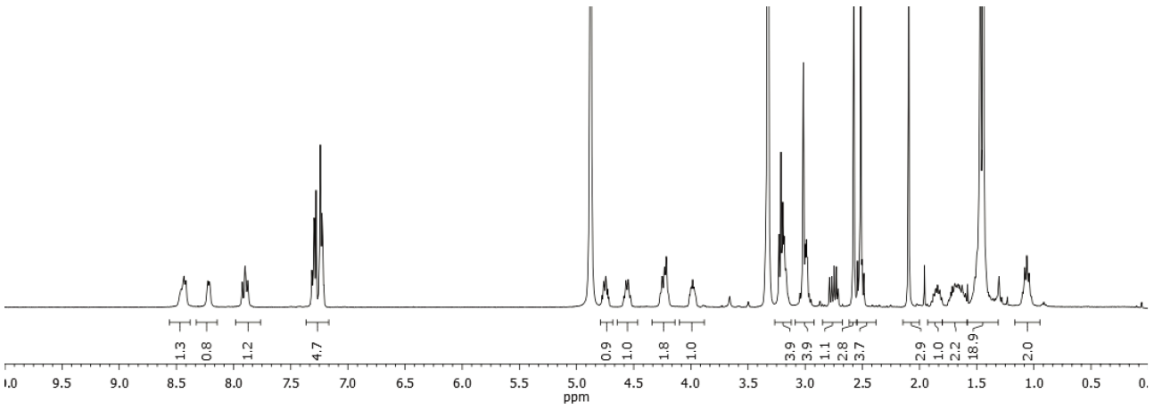

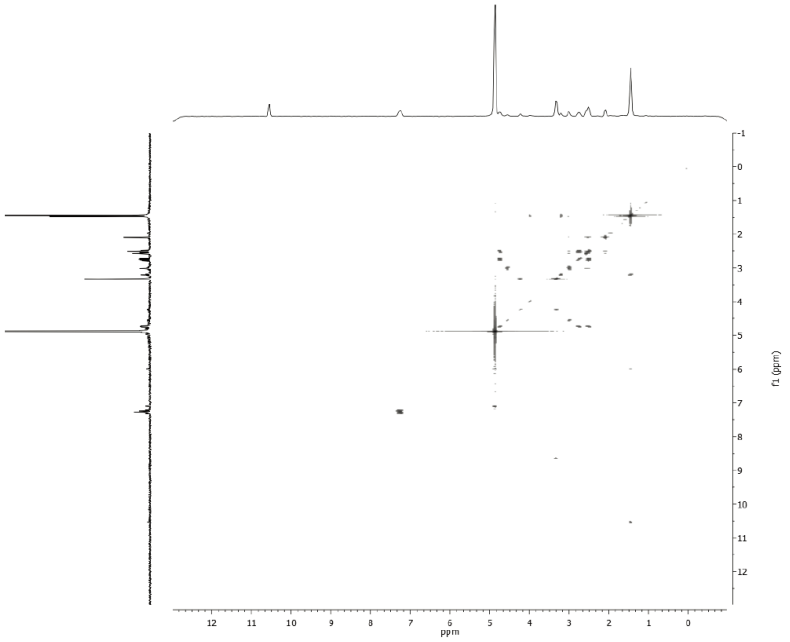

***Cyclo*[Arg-Gly-Asp-*D*-Phe-Lys(N_3)] (3a)**

^{1}H NMR 400 MHz, ^{13}C NMR 100.6 MHz, ^{1}H-^{1}H-COSY, d_6-DMSO

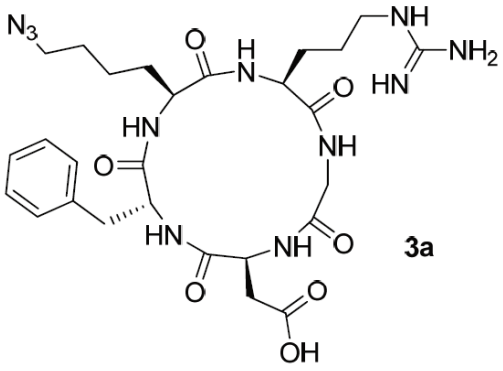

3a

Chemical Formula: $C_{27}H_{39}N_{11}O_7$
Exact Mass: 629.3034
Molecular Weight: 629.6681

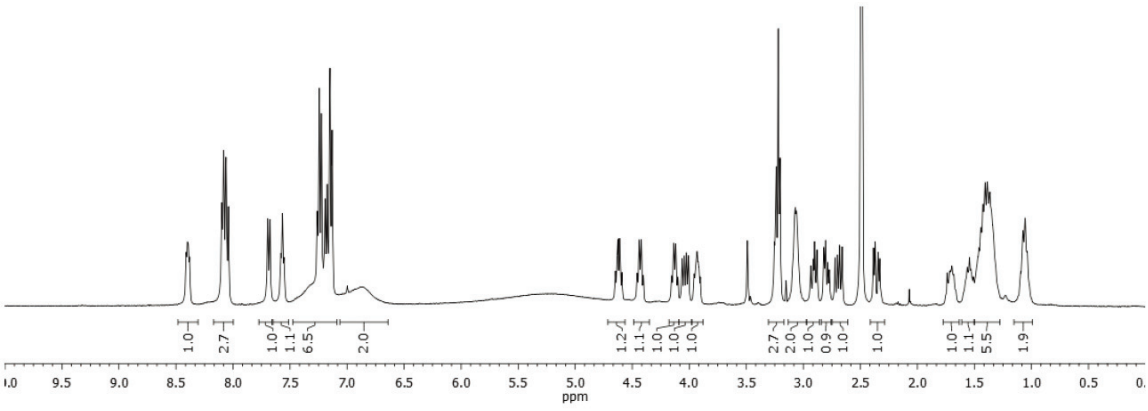

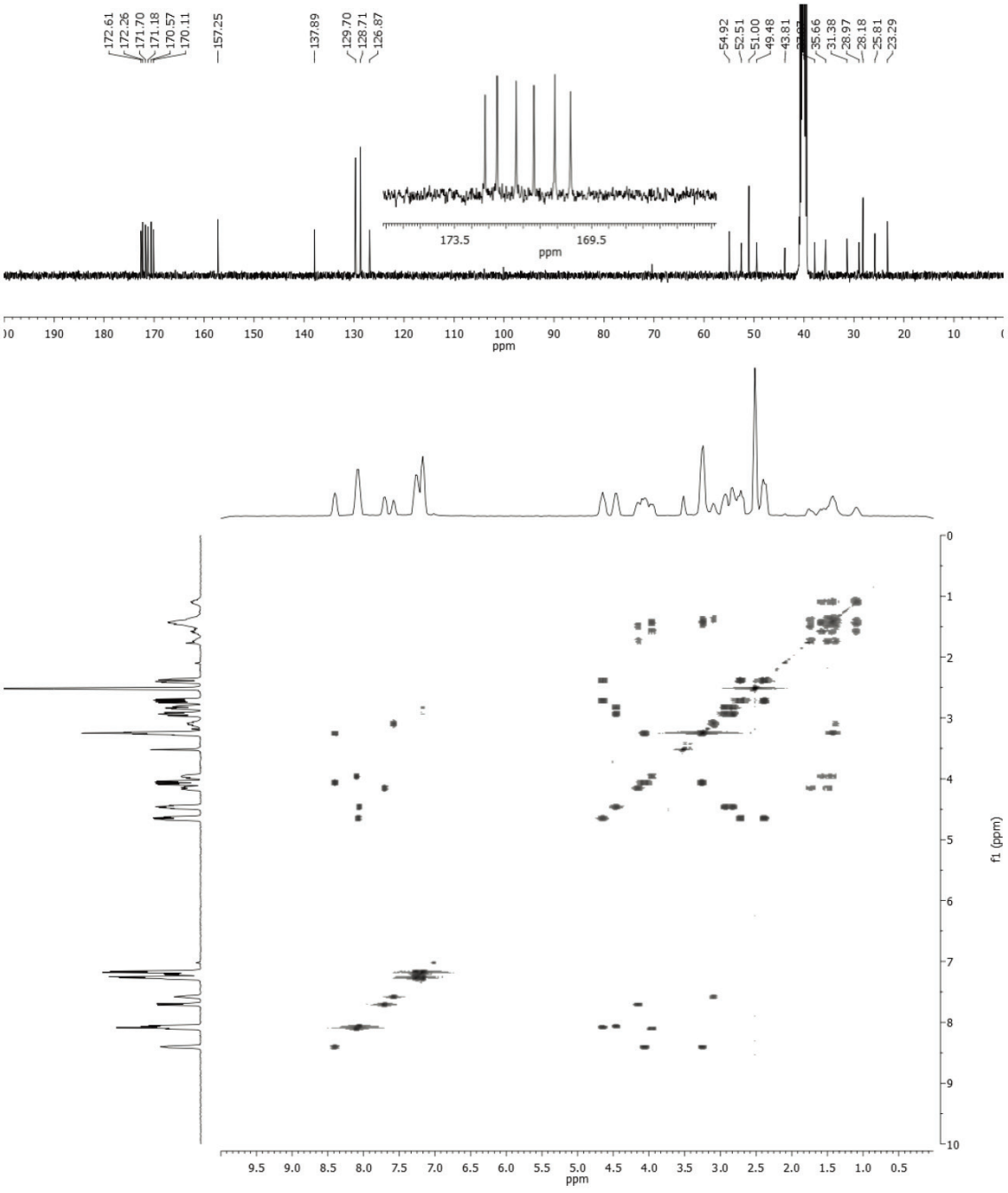
172.61
172.26
171.70
171.18
170.57
170.11
157.25
137.89
129.70
128.71
126.87
54.92
52.51
51.00
49.48
43.81
35.66
31.38
28.97
28.18
25.81
23.29
173.5
169.5
ppm
ppm
f1 (ppm)

***N*-Tritylpiperazine**

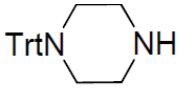

Chemical Formula: $C_{23}H_{24}N_2$
Exact Mass: 328.1939
Molecular Weight: 328.4501

^{1}H NMR 400 MHz, ^{13}C NMR 100.6 MHz, CD_2Cl_2

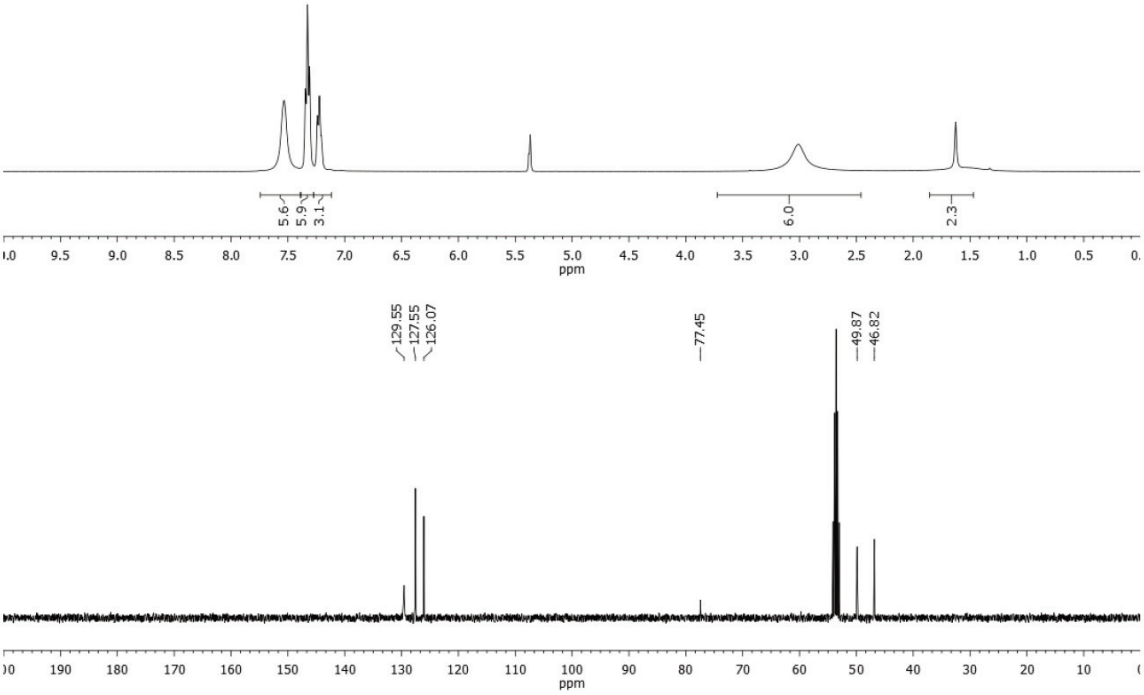

Mono-*tert*-butyl succinate

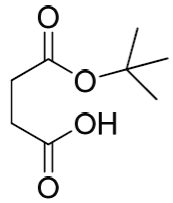

Chemical Formula: $C_8H_{14}O_4$
Exact Mass: 174.0892
Molecular Weight: 174.1944

^{1}H NMR 300 MHz, ^{13}C NMR 75.5 MHz, $CDCl_3$

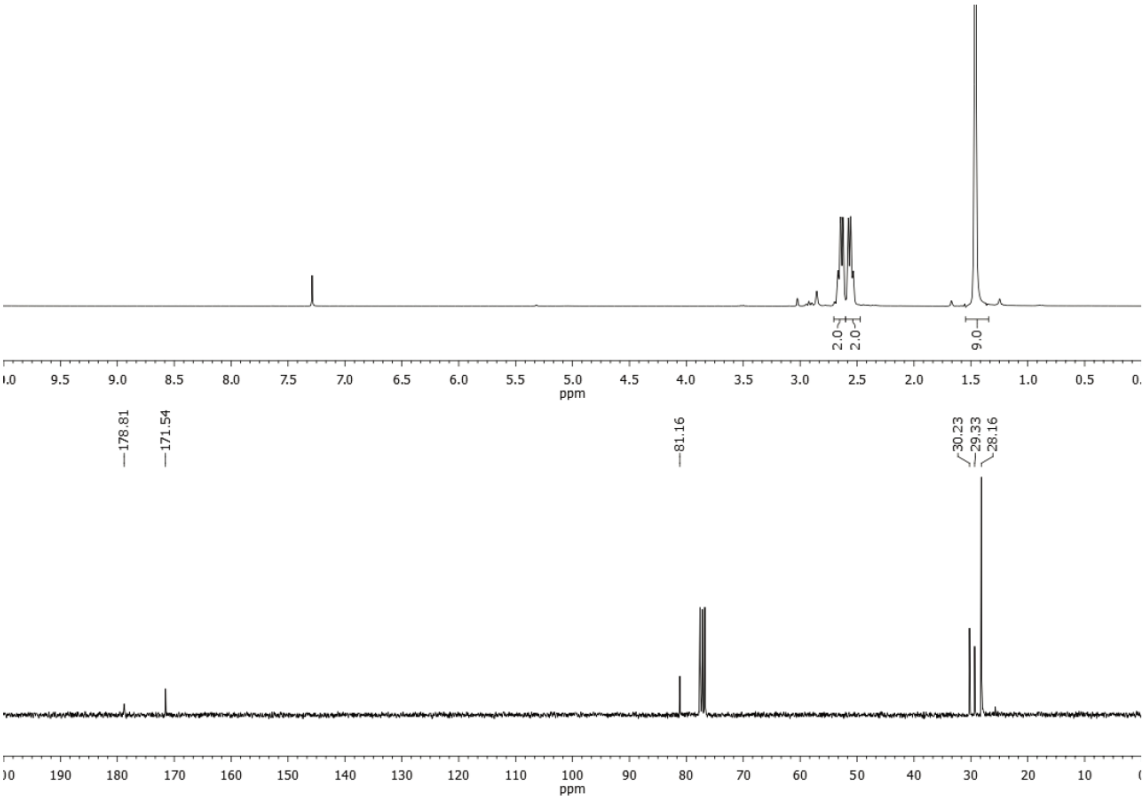

***Tert*-butyl 4-oxo-4-(4-tritylpiperazin-1-yl)butanoate (4)**

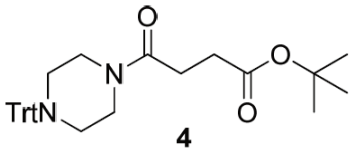

4

Chemical Formula: $C_{31}H_{36}N_2O_3$
Exact Mass: 484.2726
Molecular Weight: 484.6291

^{1}H NMR 400 MHz, ^{13}C NMR 100.6 MHz, CD_2Cl_2

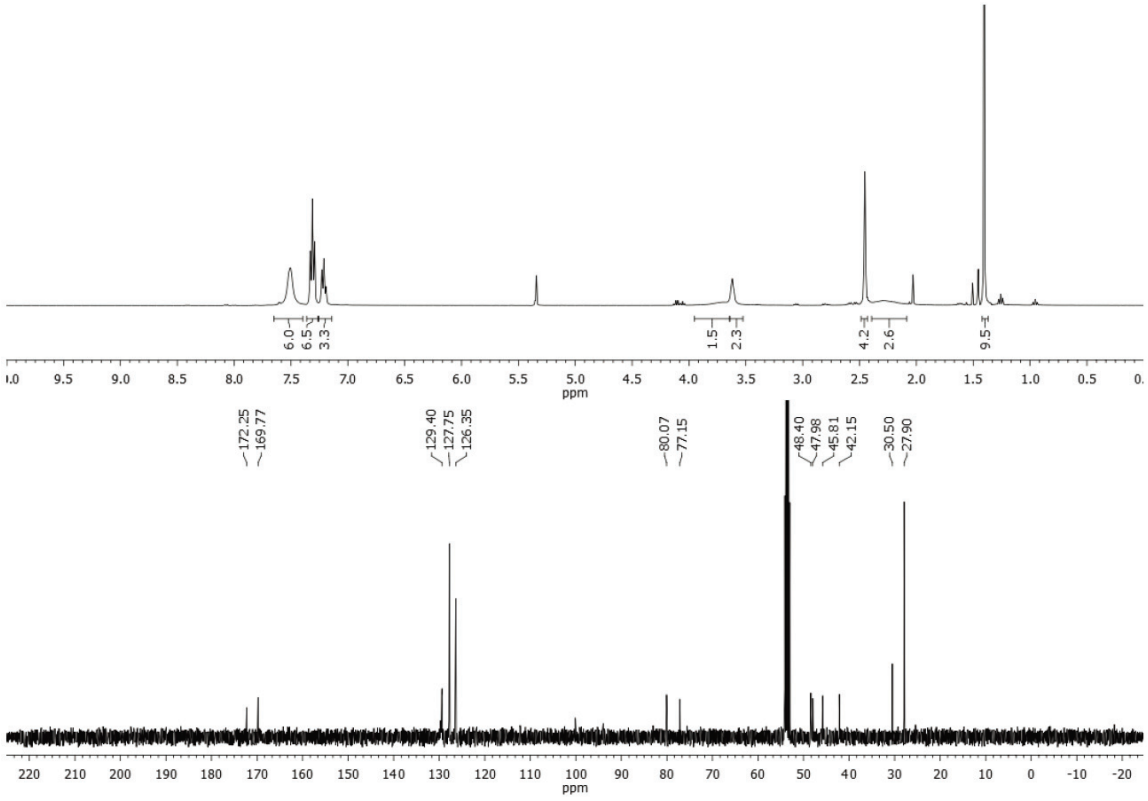

***Tert*-butyl 4-oxo-4-(piperazin-1-yl)butanoate (5)**

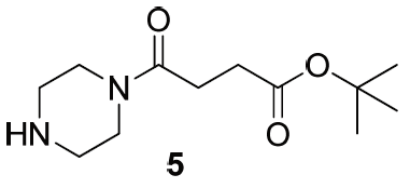

5

Chemical Formula: $C_{12}H_{22}N_2O_3$
Exact Mass: 242.1630
Molecular Weight: 242.3147

^{1}H NMR 400 MHz, ^{13}C NMR 100.6 MHz, $CDCl_3$

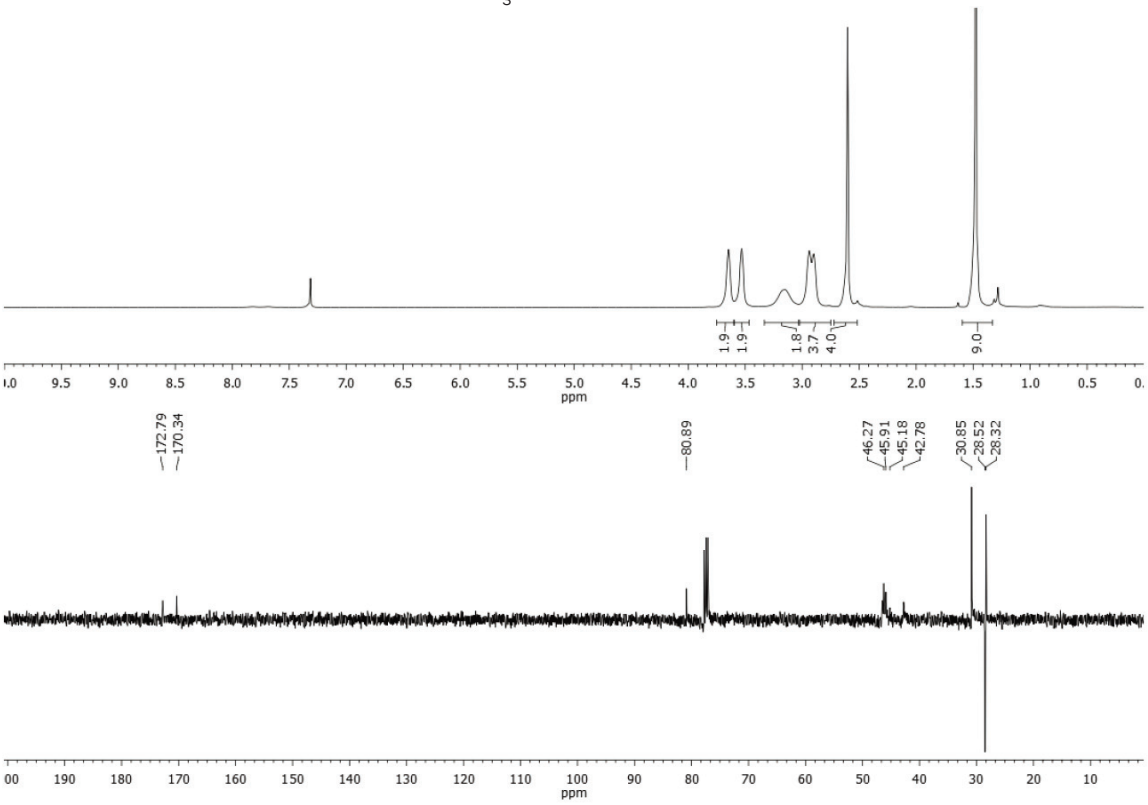

***Tert*-butyl 4-oxo-4-(4-(2,4,6-trifluoro-3-(4,4,5,5-tetraphenyl-1,3,2-dioxaborolan-2-yl) benzoyl)piperazin-1-yl)butanoate (6)**

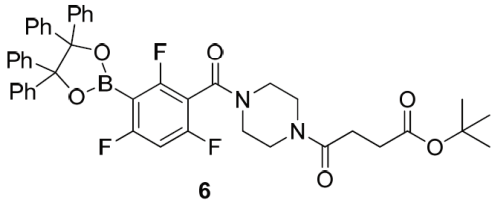

6

Chemical Formula: $C_{45}H_{42}BF_3N_2O_6$
Exact Mass: 774.3088
Molecular Weight: 774.6310

^{19}F NMR 282.4 MHz, ^{1}H NMR 400 MHz, ^{13}C NMR 100.6 MHz, CD_2Cl_2

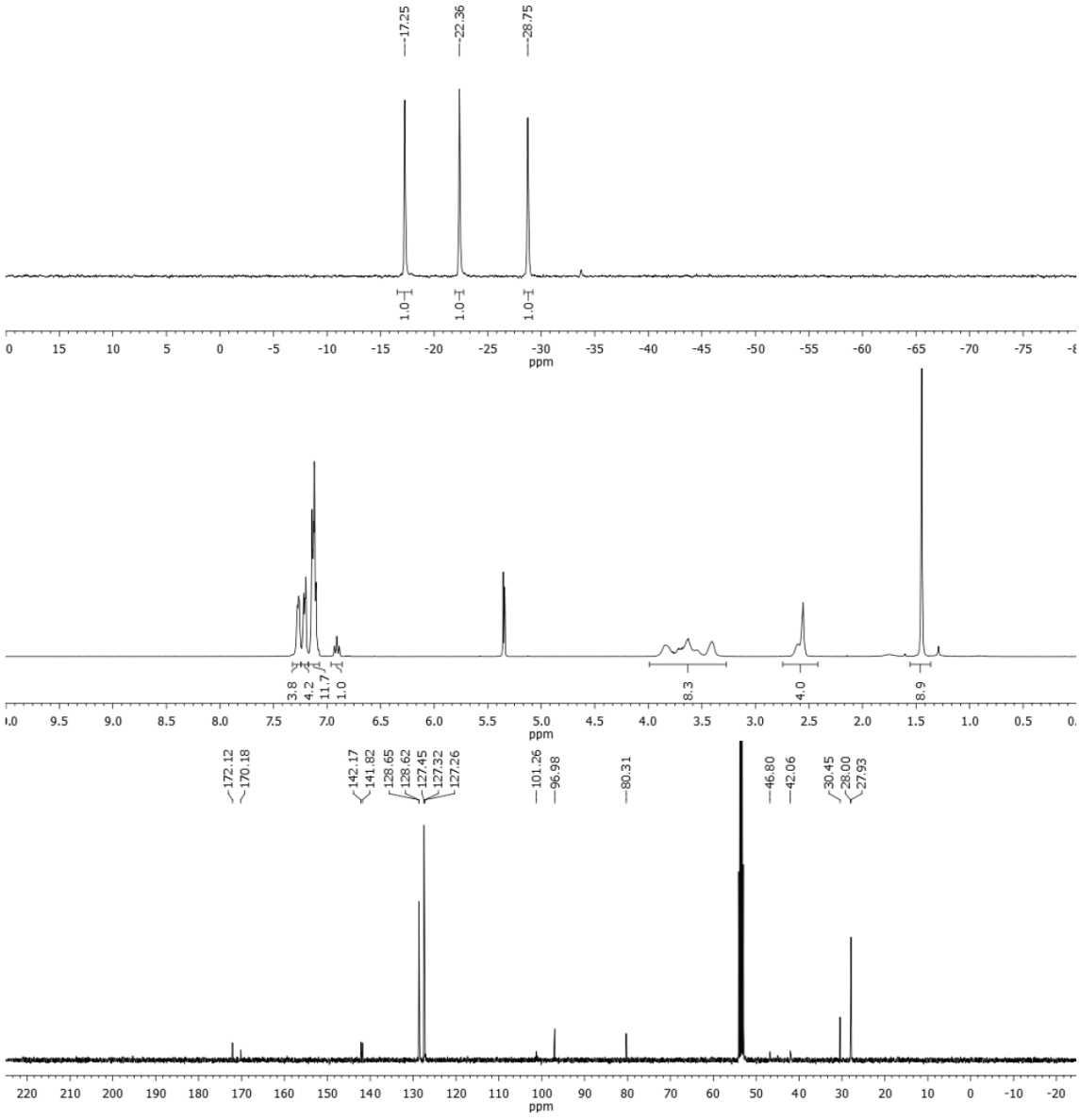

4-Oxo-4-(4-(2,4,6-trifluoro-3-(4,4,5,5-tetraphenyl-1,3,2-dioxaborolan-2-yl)benzoyl) piperazin-1-yl)butanoic acid (7)

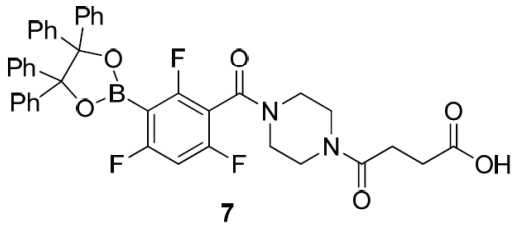

7

Chemical Formula: $C_{41}H_{34}BF_3N_2O_6$
Exact Mass: 718.2462
Molecular Weight: 718.5247

^{19}F NMR 282.4 MHz, ^{1}H NMR 400 MHz, ^{13}C NMR 100.6 MHz, CD_2Cl_2

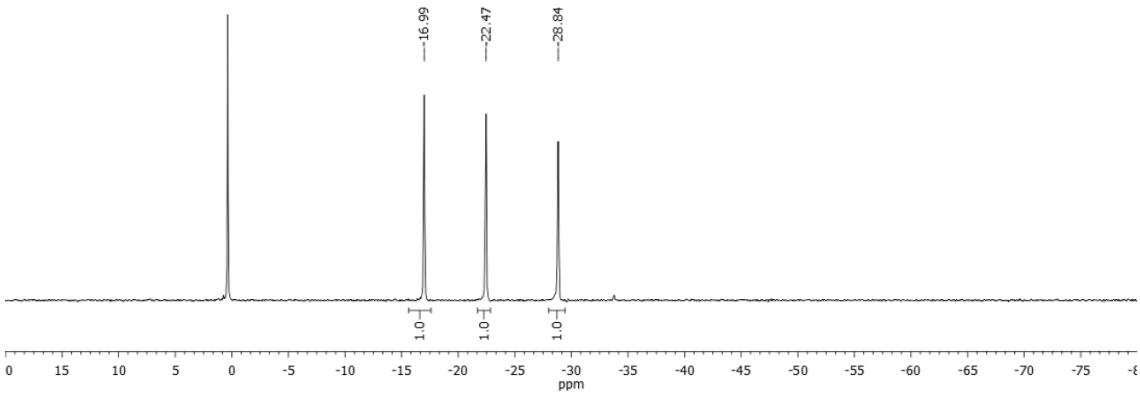

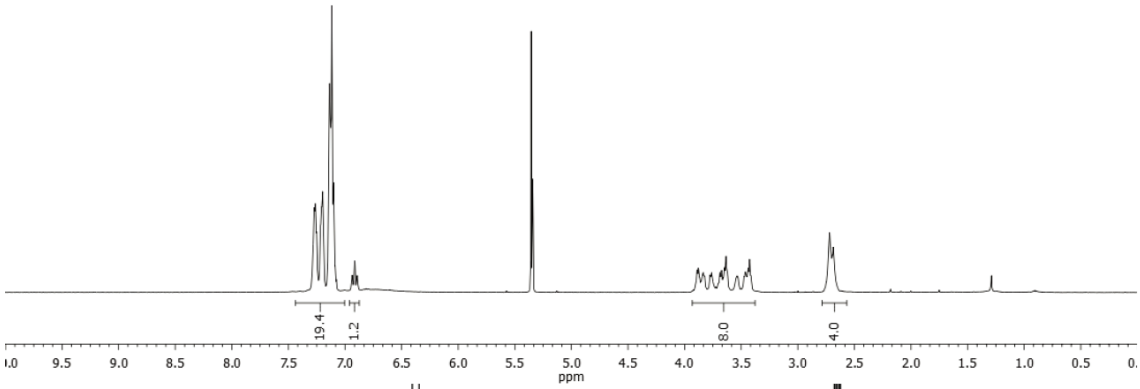

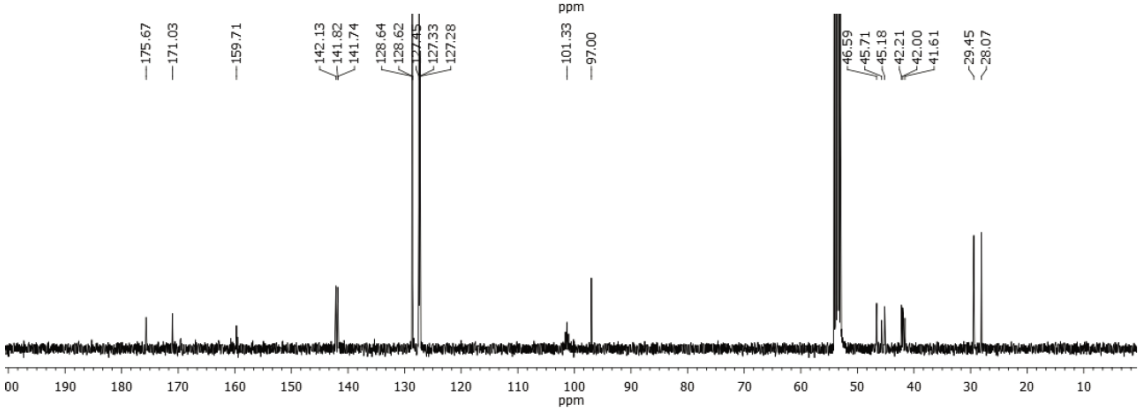

***Cyclo*[Arg-Gly-Asp-*D*-Phe-Lys(piperazinyl-boronate)] (9)**

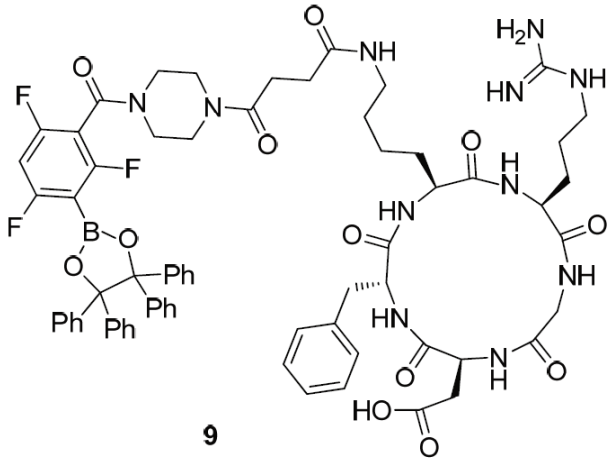

9

Chemical Formula: $C_{68}H_{73}BF_3N_{11}O_{12}$
Exact Mass: 1303.5485
Molecular Weight: 1304.1799

^{19}F NMR 282.4 MHz, ^{1}H NMR 400 MHz, ^{13}C NMR 100.6 MHz, d_4-MeOD

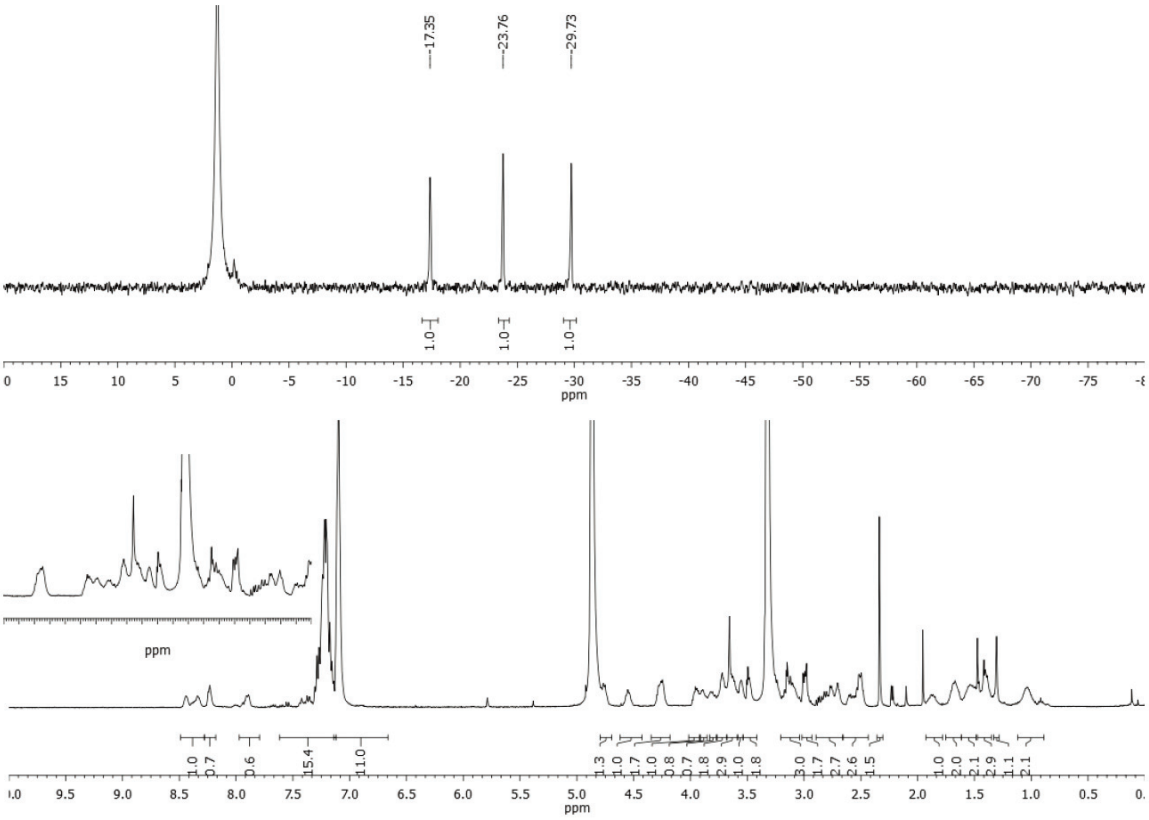

***Cyclo*[Arg-Gly-Asp-*D*-Phe-Lys(suc-piperazinyl-ArBF$_3$)] (10)**

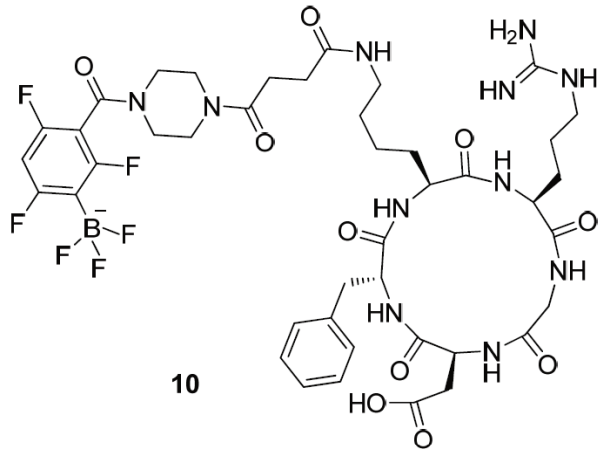

10

Chemical Formula: $C_{42}H_{53}BF_6N_{11}O_{10}^-$
Exact Mass: 996.3980
Molecular Weight: 996.7399

^{19}F NMR 282.4 MHz, d_6-DMSO

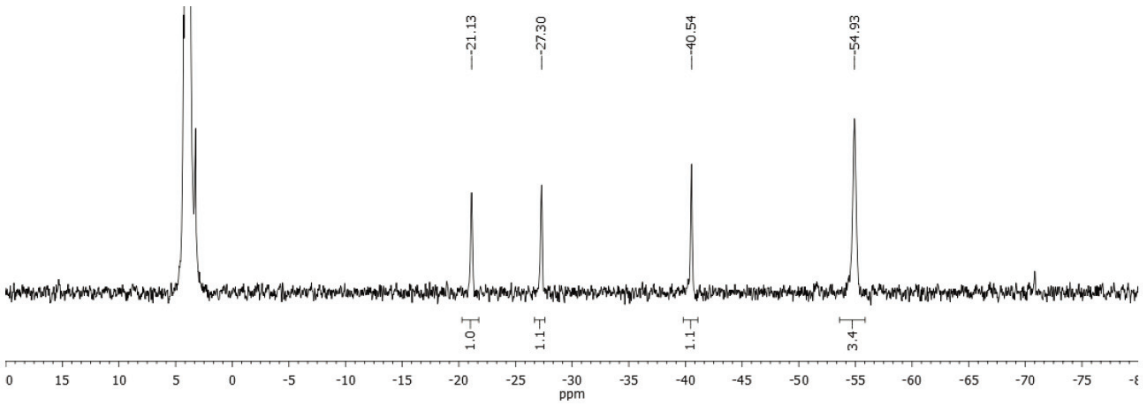

2,4,6-Trifluoro-3-(1*H*-naphtho[1,8-de][1,3,2]diazaborinin-2(3*H*)-yl)benzoic acid (11)

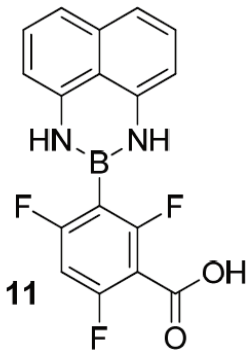

11

Chemical Formula: $C_{17}H_{10}BF_3N_2O_2$
Exact Mass: 342.0787
Molecular Weight: 342.0797

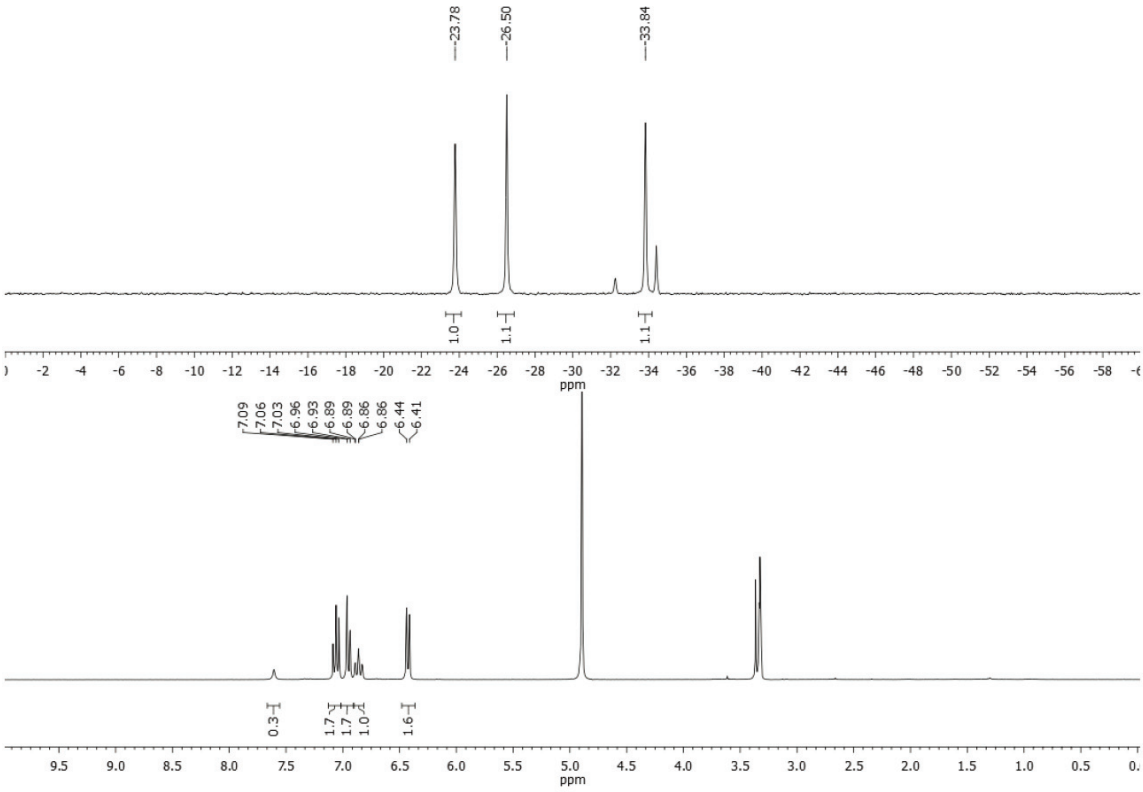

Alkynylborimidine (12)

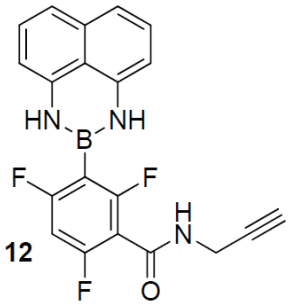

Chemical Formula: $C_{20}H_{13}BF_3N_3O$
Exact Mass: 379.1104
Molecular Weight: 379.1429

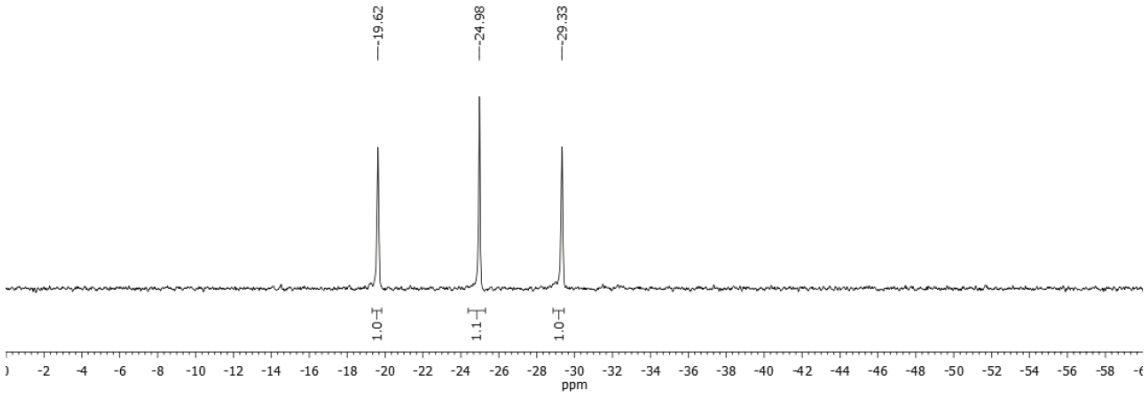

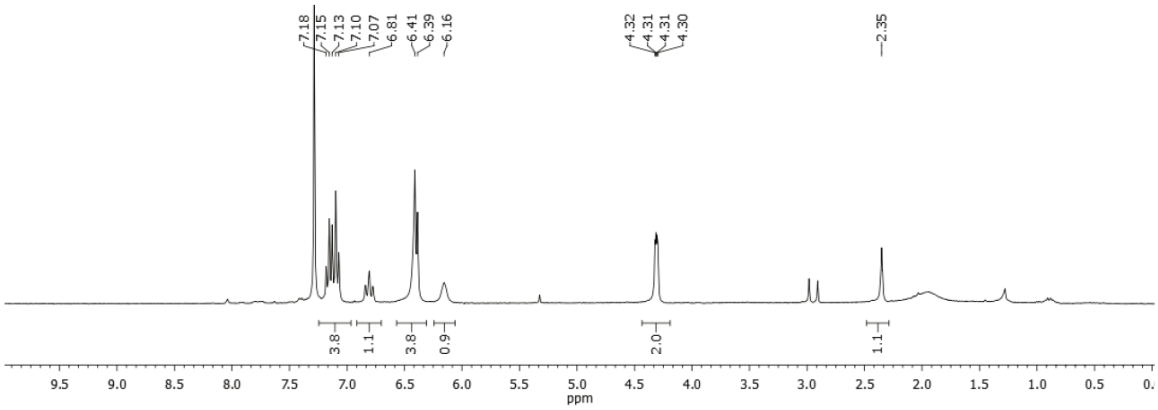
7.18
7.15
7.13
7.10
7.07
6.81
6.41
6.39
6.16
4.32
4.31
4.31
4.30
2.35
3.8
1.1
3.8
0.9
2.0
1.1
9.5 9.0 8.5 8.0 7.5 7.0 6.5 6.0 5.5 5.0 4.5 4.0 3.5 3.0 2.5 2.0 1.5 1.0 0.5
ppm